SSC-SR-1030
(SSC-MAG-C-201)

SSC MAGNET SYSTEM: STRESS ANALYSIS FOR SEISMIC AND TRANSPORTATION LOADINGS

September 1987

Prepared for:

Magnet Division
Universities Research Association
Berkeley, CA

EQE Incorporated/Corporate Office
595 Market Street, 18th Floor
San Francisco, CA 94105
Telex 296166/(415) 495-5500

3300 Irvine Avenue
Newport Beach, CA 92660
(714) 852-9299

Two Annabel Lane, Ste. 101
San Ramon, CA 94583
(415) 866-1766

SSC MAGNET SYSTEM: STRESS ANALYSIS FOR SEISMIC AND TRANSPORTATION LOADINGS

September 1987

Prepared for:

Magnet Division
Universities Research Association
Berkeley, CA

Prepared by:

James J. Johnson
Brian J. Benda
David J. Doyle

EQE Incorporated
Two Annabel Lane, Suite 101
San Ramon, CA 94583

TABLE OF CONTENTS

Page

1.0 INTRODUCTION 1-1

2.0 ANALYSIS APPROACH 2-1

2.1 COLD MASS ASSEMBLY MODEL 2-1

2.2 SUSPENSION SYSTEM MODEL 2-3

2.2.1 Re-entrant Post Model 2-3

2.2.2 Center Cradle Model 2-4

2.2.3 Outboard Cradle Model 2-5

2.3 MAGNET INTERCONNECTION REGION 2-5

2.4 VACUUM VESSEL 2-6

2.5 MAGNET SYSTEM MODELS 2-7

2.5.1 Single Magnet Seismic Model 2-7

2.5.2 Piggyback Seismic Model 2-7

2.5.3 Transportation Model 2-8

3.0 DYNAMIC RESPONSE ANALYSES AND RESULTS 3-1

3.1 DYNAMIC CHARACTERISTICS OF THE MAGNET SYSTEM MODELS 3-1

3.2 RESPONSE TO SEISMIC EXCITATION 3-2

3.2.1 RG 1.60 Design Ground Response Spectra 3-2

3.2.2 Site Specific Design Spectra Response 3-4

3.3 RESPONSE TO TRANSPORTATION LOADING 3-8

4.0 SUMMARY AND RECOMMENDATIONS 4-1

4.1 STRESS SUMMARY 4-1

4.2 RECOMMENDATIONS 4-3

4.3 POTENTIAL DESIGN MODIFICATIONS 4-5

5.0 REFERENCES 5-1

LIST OF TABLES

2.1 Cold mass Assembly and Vacuum Vessel Structural Parameters 2-9

2.2a Geometry and Material Properties for Inner Post 2-10

2.2b Geometry and Material Properties for Outer Post 2-11

2.2c Geometry and Material Properties for Tie Bars 2-12

2.3 End Connection/Support Post Stiffness Comparison 2-13

3.1 Characteristic Modes of the Single Magnet Seismic Model 3-10

3.2 Characteristic Modes of the Cold Mass/ Support Systems 3-11

3.3 Characteristic Modes of the Piggyback Configuration 3-12

3.4 Characteristic Modes of the Transportation Model 3-13

3.5 Support Post Maximum Combined Membrane and Bending Stresses, Seismic Excitation, RG 1.60 Design Spectra 3-14

3.6 Support Post Maximum Combined Membrane and Bending Stresses, Seismic Excitation, Soft Soil Design Spectra, Surface-Founded 3-15

3.7 Support Post Maximum Combined Membrane and Bending Stresses, Seismic Excitation, Soft Soil, Design Spectra, Founded at -30 Ft. 3-16

3.8 Support Post Maximum Combined Membrane and Stresses, Transportation Excitation, Half-Sine Pulse Design Spectra 3-17

LIST OF FIGURES

1-1 Isometric View of the Cryostat System 1-4

1-2 Section View of Cryostat System 1-5
2-1 Cold Mass Assembly 2-14
2-2 Results of Cold Mass Stiffness Test Conducted by Fermilab 2-15
2-3 Cold Mass Support Assembly 2-16
2-4 Re-entrant Post Design 2-17
2-5 Schematic of Support Post Finite Element Model 2-18
2-6 Stiffness Matrix for Re-entrant Post 2-19
2-7 Schematic of Center Cradle Finite Element Model 2-20
2-8 Stiffness Matrix for Center Cradle 2-21
2-9 Schematic of Outboard Cradle Finite Element Model 2-22
2-10 Stiffness Matrix for Outboard Cradle 2-23
2-11 Structural Components of Cold Mass Support System 2-24
2-12 Schematic of Substructure Approach 2-25
2-13 Single Magnet Seismic Model 2-26
2-14 Piggyback Seismic Model 2-27
2-15 Section View of Vacuum Vessel Support 2-28
2-16 Stiffness Matrix for Support Ring 2-29
2-17 External Axial Transportation Restraint 2-30
2-18 Stiffness Matrix for Axial Transportation Restraint 2-31
2-19 Transportation Model 2-32
3-1 Design Response Spectrum RG 1.60 Scaled to 0.3g 3-18
3-2 Site Specific Response Spectra at Surface (Six Components) 3-19
3-3 Mean and Mean-Plus-One-Standard-Deviation Response Spectra at Surface 3-20
3-4 Schematic of FLUSH Finite Element Model 3-21

3-5 Site Specific Response Spectra at -30 Ft. (Six Components) 3-22
3-6 Mean and Mean-Plus-One-Standard-Deviation Response Spectra at -30 ft. 3-23
3-7 Comparison of Mean-Plus-One-Standard-Deviation Spectra with RG 1.60 3-24
3-8 Typical Impulse Shock Loads for Various Environments 3-25
3-9 Half-Sine Pulse Response Spectrum for Axial Direction 3-26
3-10 Half-Sine Pulse Response Spectrum for Lateral Direction 3-27
3-11 Half-Sine Pulse Response Spectrum for Vertical Direction 3-28

1.0 INTRODUCTION

The superconducting magnet cryostat is a critical component of the Superconducting Super Collider (SSC). Its function is to provide high quality magnetic fields to confine and steer proton beams along circular orbits approximately 52 miles in circumference, provide low thermal loads to the refrigeration system, operate with high reliability, and be capable of mass production at a low cost.

The cryostat general arrangement is as shown in Figs. 1-1 and 1-2. The major elements of the cryostat are the cold mass assembly, cryogenic piping, suspension system, thermal shields, insulation, vacuum vessel and interconnection region. The cold mass consists of the beam tube and magnet system within a steel, cylindrical containment shell. Two thermal shields, operating independently at 20K and 80K, surround the cold mass assembly to absorb the radiant heat flux from warmer regions of the cryostat and to provide heat sink stations for the suspension system. Within the thermal shields, cryogenic piping interconnects the magnet refrigeration system throughout the circumference of the ring. The cold mass and thermal shields are supported by posts constructed as a nested pair of thin-walled fiberglass-epoxy tubes. These folded posts are located at five points along the length of each magnet segment. The entire assembly is housed within a stainless steel cylindrical vessel that defines the insulating vacuum space and provides support connection for magnet installation. The interconnection region at magnet ends provides the required mechanical and electrical connections between segments.

Conditions that control and affect cryostat design include transient, steady state and upset operation. Component design issues include fluid flow, material performance, structural integrity, displacement tolerances, and thermal performance. In addition to operating loads, structural requirements dictate that the magnet assembly shall withstand seismic, transportation, and handling and installation loads. Seismic and transportation loads are specified as follows:

- Seismic
    - Horizontal and vertical design ground response spectra of US NRC Regulatory Guide 1.60 scaled by 0.3. This represents an earthquake with 0.3g peak ground acceleration in the two horizontal directions and a corresponding 0.2g peak ground acceleration in the vertical direction.
    - Horizontal and vertical design ground response spectra for a typical soft soil site with the magnet system founded at the ground surface. This represents an earthquake whose peak ground acceleration is 0.3g in both horizontal directions and 0.2g in the vertical direction.
    - Horizontal and vertical design ground response spectra for a typical soft soil site with the magnet system founded in a tunnel at a 30 foot depth. The motion at depth corresponds to the surface motion for a typical soft soil site as discussed above. The peak accelerations and frequency content of the motion at depth differ from the surface. For a surface motion with the peak ground acceleration of 0.3g in the horizontal direction, the at depth horizontal peak acceleration is 0.27g with lower frequency content.
- Transportation

Vertical	2.0g
Lateral	1.0g
Axial	1.5g

Reference 1, the SSC collider magnet system design requirements, specifies structural loading conditions and their combination for design purposes. Also, Ref. 1 itemizes allowable stresses. In general, stresses due to seismic and transportation loading conditions by themselves and combined with dead load stresses are

provided for comparison with the allowables. Only this load combination is considered here. Reference 1 itemizes several load combinations involving seismic stresses which must be considered to make conclusive statements concerning seismic capability of the magnet system.

EQE, Inc. has conducted dynamic analyses of the Superconducting Super Collider magnet system given seismic and transportation loadings. The balance of this report, which documents this analysis effort, is organized as follows:

Section 2 identifies the analysis approach and describes the models developed for each of the major cryostat components. Section 3 describes the dynamic response analyses and the results obtained. Section 4 presents discussions and conclusions.

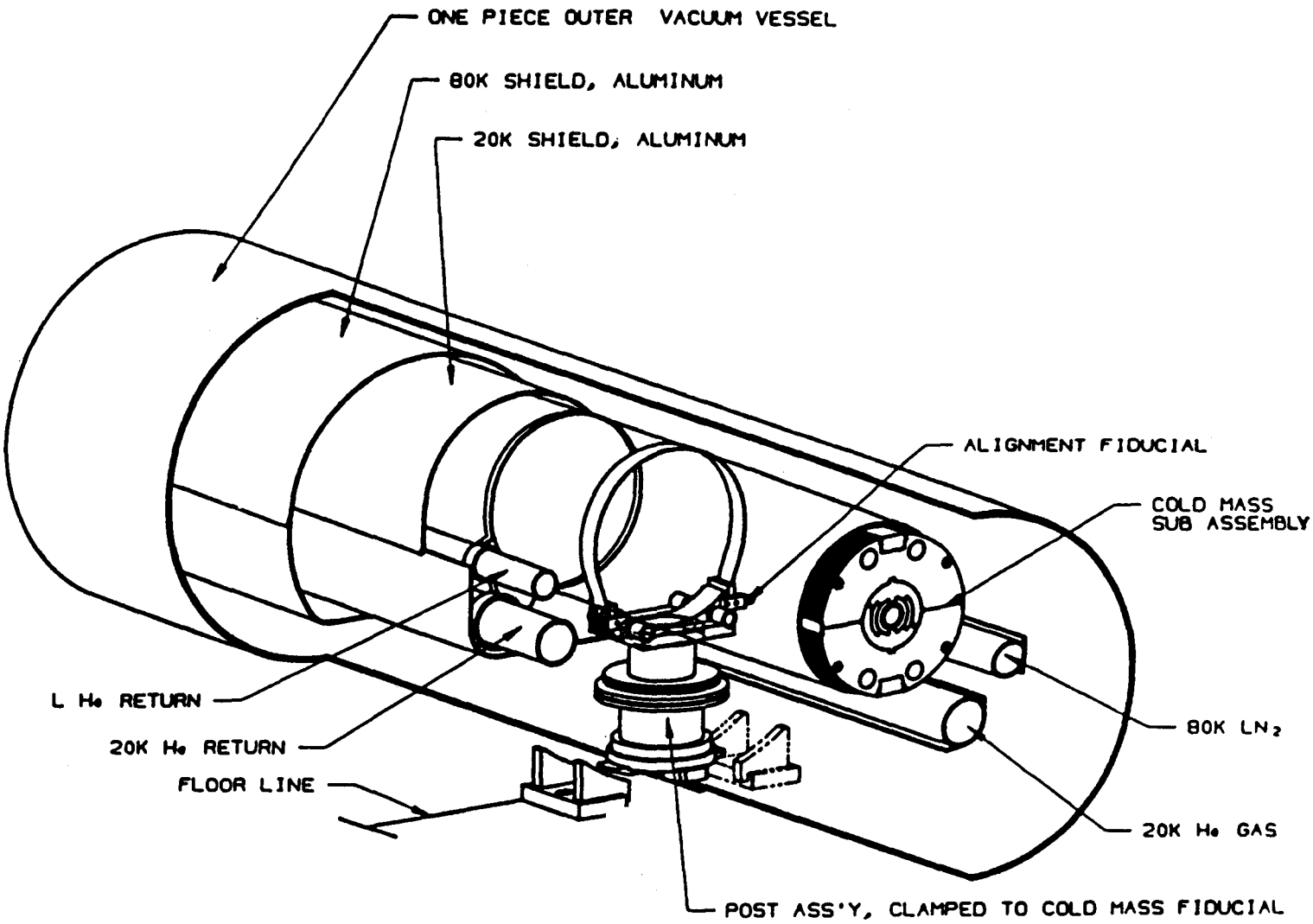

Fig. 1-1: Isometric View of the Cryostat System

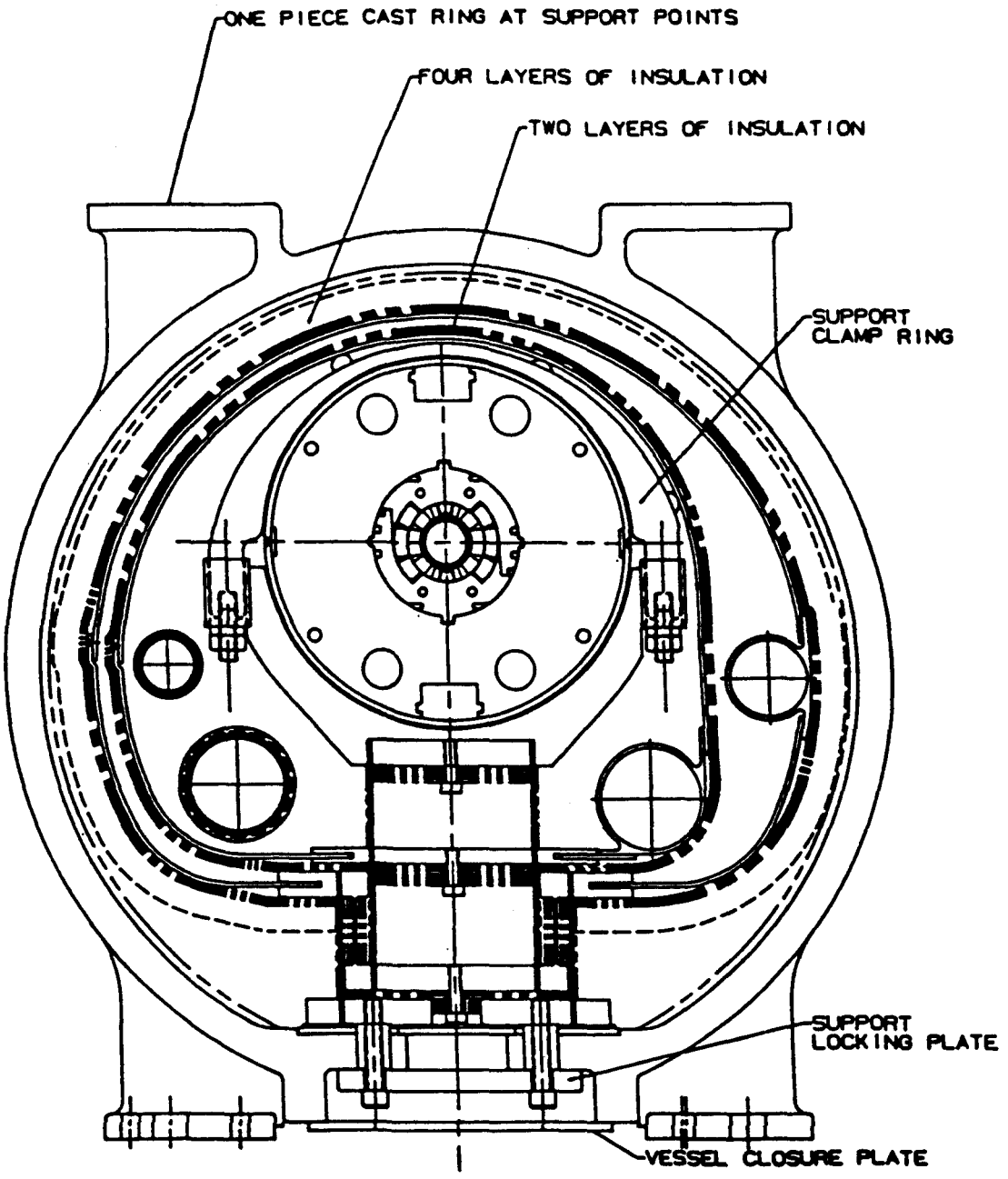

Fig. 1-2: Section View of Cryostat System

2.0 ANALYSIS APPROACH

The purpose of the dynamic analyses performed herein is to determine the response of major SSC components to the vibration and shock loading dictated by the seismic and transportation environments. As such, the analysis must include those components that define the dynamic response of the overall system. Following a review of design drawings and discussions with engineers at Fermi National Accelerator Laboratory (Fermilab), the cold mass, the support posts and cradles, the vacuum vessel and its supporting rings, the axial transportation restraints, and the bellows interconnection between magnet segments were identified as those components which most significantly affect the response of the magnet system.

The varied nature of the components' characteristics lends itself to a substructure approach to analyzing the magnet system. For components with simple geometries whose dynamic characteristics can be easily represented, less sophisticated mathematical models are constructed. For components with complex geometries or those that significantly contribute to magnet response, detailed mathematical models are constructed. These detailed models are initially used to define the stiffness characteristics of the respective components. The stiffness representations are combined with the less-sophisticated models of other components to form a simplified model of the magnet system - a model capable of determining overall response to seismic or transportation excitations. The forces and displacements obtained with the simplified model are subsequently applied to the detailed component models to recover detailed stress information. Descriptions of the models developed for each of the significant magnet components are given in the following subsection.

2.1 COLD MASS ASSEMBLY MODEL

The cold mass assembly consists of the beam tube, cos θ collared coils, stacked iron yoke laminations, outer helium containment shell and alignment fiducials; all joined together to provide a leak tight welded assembly. A cross section of the cold mass assembly is shown in Fig. 2-1.

The helium containment shell is the principal structural element of the cold mass assembly and provides the necessary rigidity between suspension posts. The structural parameters of the cold mass assembly are listed in Table 2.1.

In modeling the cold mass assembly, beam behavior is adequate to define overall response to both seismic and transportation loading. Modeling the cold mass with beam elements and assuming the system is fixed at support locations, the lowest modes of vibration have frequencies in excess of 25 Hz. This compares with dominant seismic excitation frequencies from 2 Hz to 10 Hz. The assembly is structurally rigid compared to the frequency content of the earthquake excitation. Even for higher frequency transportation loadings, beam behavior will suffice. The beam tube, magnets, laminated collar and iron yoke will significantly increase the frequencies associated with local shell modes.

Beam elements, then, were selected to model the cold mass assembly in our analyses. Twenty-one nodes and twenty elements along the length of a cold mass segment were used.

The bending stiffness of the cold mass assembly was determined at Fermilab through both analysis and test [2]. Initially, only the helium containment shell was assumed to be effective structurally. Given the section properties of the cylindrical shell, a mathematical model of the cold mass was constructed at Fermilab and subjected to a 4000 lb load as shown in Fig. 2-2. A vertical displacement of 0.292 inches was calculated. Applying a comparable 4000 lb load to a physical model of the magnet system that included iron yokes, magnets and beam tube gave a displacement of 0.241 inches. Thus the physical model dictated a bending stiffness 0.292/0.241 = 1.21 times that of the vacuum vessel alone. Axial, shear and torsional stiffness for the beams in our model were based only on the section properties of the cold mass outer steel containment shell.

In order to benchmark the cold mass model, we simulated the test conducted by Fermilab. Applying a 4,000 lb vertical load to the configuration shown in Fig. 2-2 led to a center displacement of 0.255 inches -- only a 6% difference from the test. Hence, the model was considered validated.

2.2 SUSPENSION SYSTEM MODEL

The cold mass assembly and thermal shields are supported relative to the vacuum vessel by the suspension system. This system must function under conditions that include cryostat assembly, shipping and installation, magnet cooldown and warm up, steady-state operations and upset conditions.

The cold mass and shield assemblies are supported at five points along their length. The number and location of supports was determined by Fermilab as a compromise between the need to minimize supports for reasons of magnet fabrication and alignment ease and the need to minimize cold mass deflection between support points. To allow axial thermal expansion, only the center post provides axial restraint. Each of these five supports is supported on the vacuum vessel. At two of the five locations, the vacuum vessel is supported to ground. At the other three, the vacuum vessel is stiffened but not supported to ground.

A re-entrant or "folded" post design is used to support the cold mass assembly. A post support resists load through compression of the feet on the vessel supporting rings (for two posts), and through bending of the vacuum vessel itself for the other three. However, rather than using auxiliary members to resist lateral loads, the section geometry of the post acts in bending if loaded in a non-vertical direction.

The cold mass support is illustrated in Fig. 2-3. It consists of the re-entrant post itself and a cradle that surrounds the cold mass, except for the center cradle, and physically attaches the cold mass to the post. In the analyses, the support components, posts and center and outboard cradles, were individually modeled and are discussed separately below.

2.2.1 Re-Entrant Post Model

Details of the re-entrant post are given in Fig. 2-4. Its principal structural elements identified in the figure are an outer cylinder that attaches at its base to the vacuum vessel, an inner shell that attaches at its top to the cradle, and a "dog bone" cylinder that connects the bottom of the inner post to the top of the outer post. The 20K thermal shield is supported by the inner post at the post mid-length

while the 80K shield is supported at the top of the outer cylinder. The shields do not contribute to the stiffness of the posts and were not included in the model. Loads induced in the support by the cold mass are transmitted down the inner post, up the "dog bone" to the top of the outer post, then down to the vacuum vessel base.

EQE constructed a detailed model of the re-entrant post. By taking advantage of the axisymmetry of the post geometry, the support was modeled with axisymmetric shell elements in the MODSAP finite element program [3]. This element accounts for circumferential variation in loadings and response by expanding each into harmonic functions of any order. For the present case, harmonics n = o and n = 1 are used. Harmonic n = o models vertical and torsional behavior. Harmonic n = 1 models lateral behavior. Sixty-seven nodes and sixty-four elements defined the inner and outer posts as well as the "dog bone" connection. Figure 2-5 illustrates the model grid. Post geometry and material properties used in the model are summarized in Table 2.2 (a-c).

Using the detailed support model, an equivalent stiffness representation of the post was generated for use in the simplified magnet system model. Unit forces and moments were applied to the top of the inner post and displacements and rotations were calculated. A flexibility matrix was thus determined and inverted to define the overall stiffness characteristics. The post stiffness matrix is given in Fig. 2-6. The detailed post model was used subsequent to the dynamic analysis of the overall magnet system to recover local stress response.

2.2.2 Center Cradle Model

The center cradle is essentially a stiffened, curved steel plate (sweeping out approximately 120°). It is welded to a thickened center portion that fits over the top of the center post. The curved portion of the cradle is in turn welded to the bottom of the cold mass. Figure 2-7 shows the geometry and the finite element grid. The plate portion is modeled with 48 thin shell finite elements whereas the thickened center portion is made up of 56 8-node brick elements. The cradle is bolted to the post in four locations. The translational degrees of freedom at these four nodes are fixed. The cold mass was assumed to remain in contact with the surface of the cradle due to the rigidity of cold mass. This was modeled by rigidly

linking all cold mass-cradle contact areas on the cradle to a central axis representing the cold mass itself. Unit displacements were then applied to the rigidly modeled cold mass and the cradle deformed under the imposed boundary conditions in order to determine its stiffness matrix. By applying unit displacements in all six degrees-of-freedom at the top of the cradle, stiffnesses were obtained directly. The center cradle model and stiffness matrix are shown respectively in Figs. 2-7 and 2-8. This detailed cradle model was used subsequently to determine final stresses as described for the post model.

2.2.3 Outboard Cradle Model

The four outboard cradles are significantly different than the center one. The primary reason being the need to accommodate thermal contraction and expansion of the cold mass itself. Therefore, the cold mass must be able to slide axially unrestrained within the cradle perimeter; axial translations and rotations about the center axis are un-restrained. Four special polymer pads located about every 90° around the perimeter fulfill this requirement physically. Figure 2-9 shows the geometry and the finite element grid representing the outboard cradle. The cradle itself is modeled with 118 thin shell finite elements that form a closed ring around the cold mass. Only nodes which lie on the pad locations are rigidly linked to the central rigid beam, allowing the ring to deform between the pads. The outboard cradle stiffness matrix was determined as described for the center cradle. Figures 2-9 and 2-10 show the outboard cradle model as well as its stiffness matrix. Both cradles were modeled and analyzed using the SUPERSAP finite element program [4].

2.3 MAGNET INTERCONNECTION REGION

The ring of the Superconducting Super Collider is comprised of a series of linear magnet segments approximately 55 ft. in length. The segments are interconnected at their ends to form a continuous system. Metal bellows connect the beam tube, cryostat piping, cold mass containment shell, and outer vacuum vessel. The relative stiffness of the bellows connections compared to the stiffness of the cryostat system itself dictates the extent that dynamic interaction between magnet segments will occur.

To determine stiffnesses of the interconnection components, models of the cold mass vacuum vessel bellows and a cryostat piping bellows were developed. Not all data necessary to define the bellows geometry was available, but sufficient information was obtained from design drawings to construct bellows models of good accuracy. As with the re-entrant post model, the axisymmetric shell element in MODSAP was used to model the bellows. Static analyses to determine axial and lateral stiffness were conducted. Since the bellows design specification called out a required axial stiffness, a comparison between the calculated stiffness and the design value provided a benchmark as to the accuracy of the model.

Table 2.3 summarizes the analysis results. For the two bellows geometries considered, the required axial stiffness and the calculated axial and lateral stiffness are listed. The excellent agreement between the required and calculated axial stiffness confirms the accuracy of the model. In addition to bellows stiffnesses the axial and lateral stiffness of the cold mass/support post assembly is also given. The stiffness of the bellows is seen to be much less than that of the magnet system. This flexibility of the bellows isolates adjacent magnet segments, preventing any dynamic interaction between them. For this reason, the dynamic model of the magnet system used in all of the analyses needs only to include a single magnet section -- the effect of adjacent magnet segments is negligible.

2.4 VACUUM VESSEL

Since three of the posts are supported directly off the vacuum vessel at locations where there is no support to ground, the dynamic characteristics of the vessel itself must be included in all of the models. At the other two post locations, loads are taken out through the stiffened vacuum vessel support to ground. The vessel itself is modeled with 30 beam elements located at its center line. The properties of the vessel vary due to the five stiffened sections at the post locations (all five are accounted for although only two are attached directly to ground). Vacuum vessel dimensions and properties are indicated in Table 2.1 with the cold mass properties.

2.5 MAGNET SYSTEM MODELS

Three distinct models were developed for the range of loading and design criteria specified: a single-magnet seismic model, a double-magnet (piggyback) seismic model, and a single-magnet transportation model. The magnet systems in all models are identical, however, the support and boundary conditions vary between models. Figures 2-11 and 2-12 show schematically the manner in which the substructure approach applies to all three models. These three simplified models were all analyzed with the GEMINI finite element program [5].

2.5.1 Single Magnet Seismic Model

The beam models of the cold mass and vacuum vessel in addition to the stiffness representations of the support posts and cradles previously described were combined to form this model. Figure 2-13 shows this magnet system finite element representation. The two vacuum vessel nodes located at the supports were rigidly linked to fixed base nodes. These base nodes were fixed in all directions assuming anchor bolts to be adequately preloaded.

Each of the five cold mass supports, then, is modeled with two stiffness elements -- one representing the cradle; a second representing the posts, the bases of which are rigidly linked to the vacuum vessel. Elements running axially between posts reflect a current cryostat design that calls for stiffeners to connect the tops of the five cold mass supports to better distribute axial loads.

2.5.2 Piggyback Seismic Model

The piggyback model shown in Fig. 2-14 is essentially two single seismic models, one on top of the other. In order to accommodate the connection between upper and lower vacuum vessels, a stiffness matrix of the circular connecting ring which supports each vessel in two locations was developed and serves as the link between the vessels (Fig. 2-15). Local deformations of the ring were not modeled based on its lowest ovalling frequency being about 33 Hz (rigid as far as the behavior of the magnet system is concerned). In order to capture overall behavior, however, a beam model of the ring using sixteen beam elements around its circumference was

constructed. The support feet of the ring were assumed rigidly bolted, both top and bottom. In the ring analysis, the bottom two feet are fixed, while the upper two are allowed to move. However, to account for the fact that bolted to the top of the lower ring is another ring, the beam elements between these two upper nodes were assumed rigid. Forces were applied to the top of this ring generating a full flexibility matrix, which was inverted to yield the stiffness matrix (Fig. 2-16) of the ring incorporated in the piggyback model.

2.5.3 Transportation Model

The transportation model includes all elements incorporated into the single-magnet seismic model with one modification -- the inclusion of axial restraints at both ends of the magnet connecting the vacuum vessel to the cold mass. This restraint consists of a circular plate with eight stiffeners radiating outward from a circular cutout, which allows for its attachment to the cold mass. It is approximately 1-1/8" thick steel and is bolted in 24 locations: 12 around the circumference of the cut-out at the cold mass edge, and 12 at the vacuum vessel-restraint interface. Stiffnesses were developed for a circular plate with an effective center cut-out and also for the radial stiffeners which were combined and incorporated into the model as single stiffness matrix elements at both ends of the magnet. A schematic of the restraint and also its stiffness matrix are shown respectively in Figs. 2-17 and 2-18. Figure 2-19 shows the resulting model.

Table 2.1

COLD MASS ASSEMBLY AND VACUUM VESSEL STRUCTURAL PARAMETERS

COLD MASS	
Outside Diameter	10.5 in.
Length	665 in.
Weight	15750 lbs.
Containment Shell	
Material	316 SST
Thickness	0.188 in.
Axial Area	6.075 $in.^2$
Flexural Stiffness	103.10$in.^4$
Torsional Stiffness	161.48 $in.^4$
VACUUM VESSEL	
Outside Diameter	24.0 in.
Length	645 in.
Weight (including support rings)	4324 lbs.
Thickness	0.25 in.
Axial Area	18.65 $in.^2$
Flexural Stiffness	1315 $in.^4$
Torsional Stiffness	2630 $in.^4$

Table 2.2a

GEOMETRY AND MATERIAL PROPERTIES FOR INNER POST

Dimension and Direction Notation

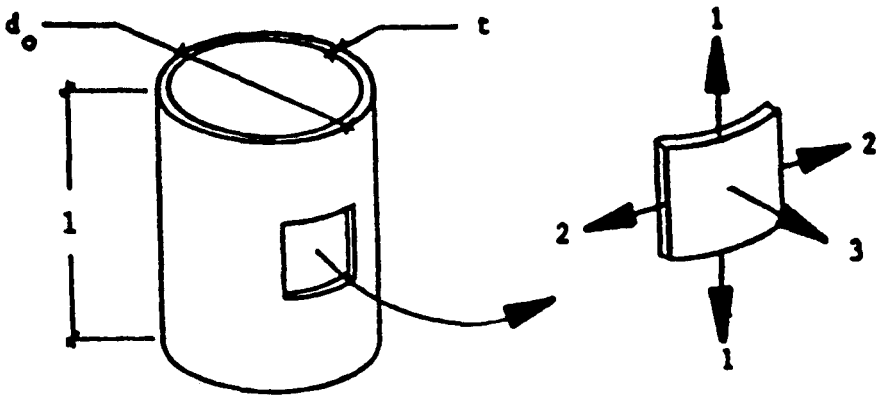

Dimensions

l (in)	:	7.310
d_o (in)	:	5.000
t (in)	:	0.129

Operating Environment

Temperature Range	:	305K → 4.5K
Relative Humidity	:	10% → 90%
Pressure Range	:	Atm → 10^{-6} Torr
Radiation Dosage	:	10^8 Rad (20 yrs)

Structural Properties @ 300K

E_1 (psi)	:	10.0×10^6	(min)
ν_1	:	0.15 → 0.25	
σ_1 (psi)	:	±60000	(min, ult)
E_2 (psi)	:	10.0×10^6	(min)
ν_2	:	0.15 → 0.25	
σ_2 (psi)	:	±60000	(min, ult)
E_3 (psi)	:	5.0×10^6	(min)
ν_3	:	0.15 → 0.25	
σ_3 (psi)	:	−60000	(min, ult)

Table 2.2b

GEOMETRY AND MATERIAL PROPERTIES FOR OUTER POST

Dimension and Direction Notation

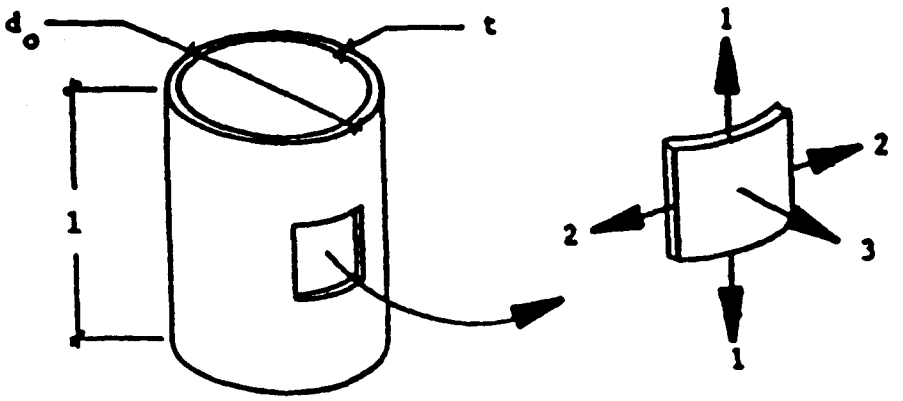

Dimensions

l (in) : 4.435
d_o (in) : 7.000
t (in) : 0.109

Operating Environment

Temperature Range : 305K → 4.5K
Relative Humidity : 10% → 90%
Pressure Range : Atm → 10^{-6} Torr
Radiation Dosage : 10^8 Rad (20 yrs)

Structural Properties @ 300K

E_1 (psi) : 4.0×10^6 (min)
ν_1 : 0.15 → 0.25
σ_1 (psi) : ±40000 (min, ult)
E_2 (psi) : 4.0×10^6 (min)
ν_2 : 0.15 → 0.25
σ_2 (psi) : ±40000 (min, ult)
E_3 (psi) : 2.0×10^6 (min)
ν_3 : 0.15 → 0.25
σ_3 (psi) : −40000 (min, ult)

Table 2.2c

GEOMETRY AND MATERIAL PROPERTIES FOR TIE BARS

Dimension and Direction Notation

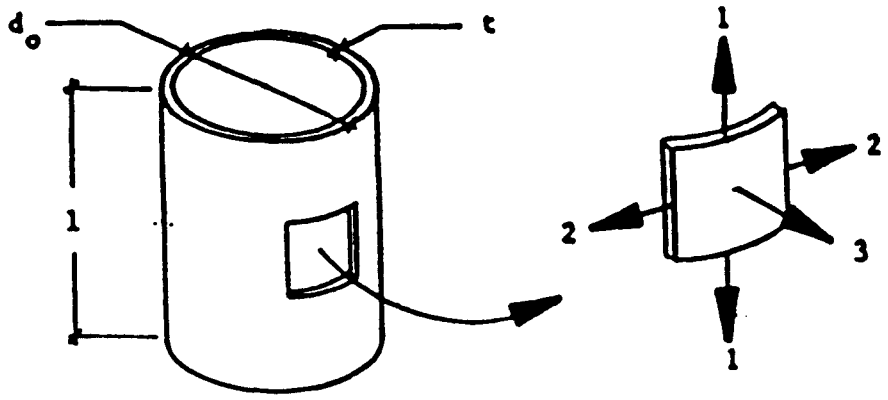

Dimensions

l (in)	:	120.0
d_o (in)	:	2.000
t (in)	:	0.250

Operating Environment

Temperature Range	:	305K → 4.5K
Relative Humidity	:	10% → 90%
Pressure Range	:	Atm → 10^{-6} Torr
Radiation Dosage	:	10^8 Rad (20 yrs)

Structural Properties @ 300K

E_1 (psi)	:	20.0×10^6	(min)
ν_1	:	0.15 → 0.25	
σ_1 (psi)	:	±60000	(min, ult)
E_2 (psi)	:	5.0×10^6	(min)
ν_2	:	0.15 → 0.25	
σ_2 (psi)	:	±15000	(min, ult)
E_3 (psi)	:	5.0×10^6	(min)
ν_3	:	0.15 → 0.25	
σ_3 (psi)	:	−60000	(min, ult)

Table 2.3

END CONNECTION/SUPPORT POST STIFFNESS COMPARISON

	Axial Stiffness (Kips/in)	Lateral Stiffness (Kips/in.)
Cold Mass Bellows		
Design Specification	1.53	-
EQE Model	1.54	3.5
LHe Return Bellows		
Design Specification	0.85	-
EQE Model	0.84	0.06
Total End Connection*	4.90	3.74
Cold Mass Supports	41.5	188.9

* Total stiffness taken as the sum of the cold mass bellows and four pipe bellows

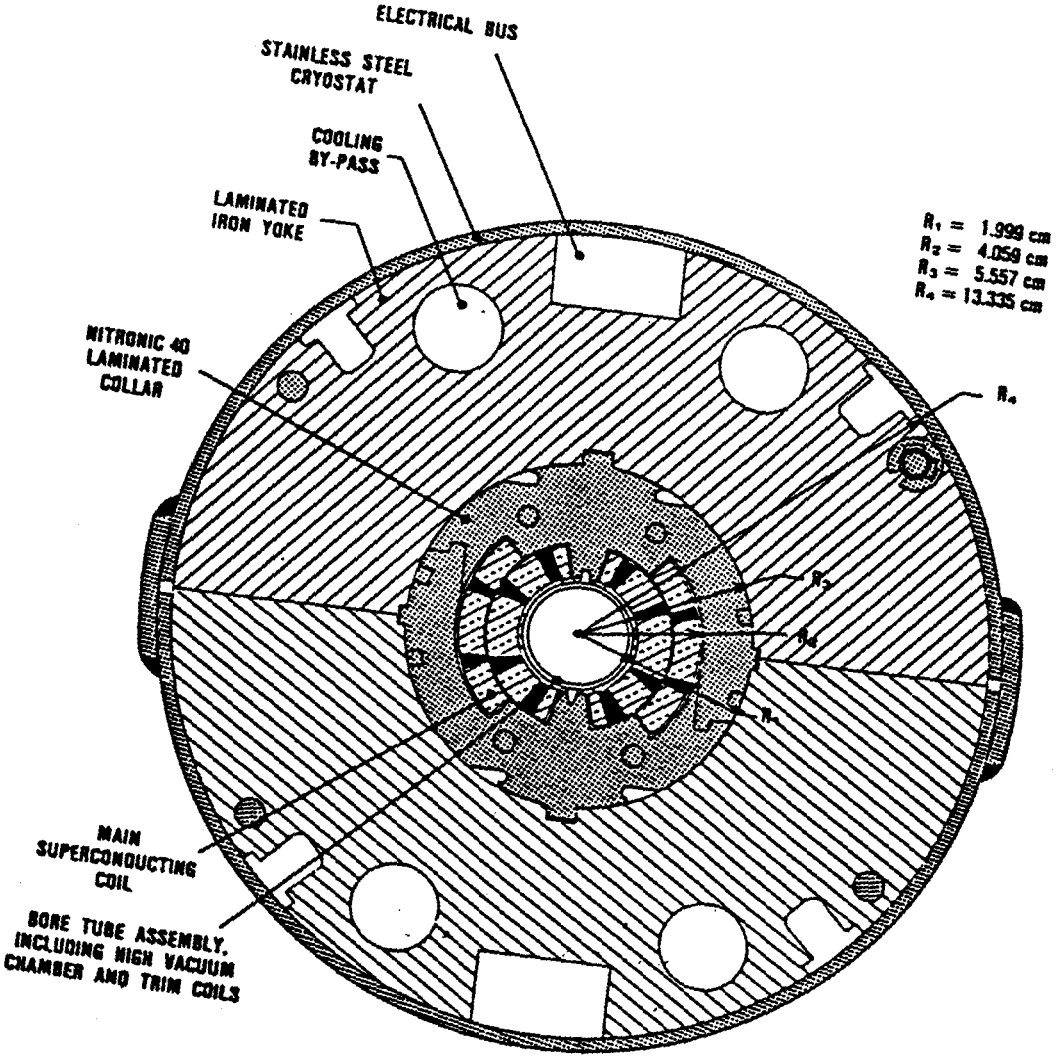

Fig. 2-1: Cold Mass Assembly

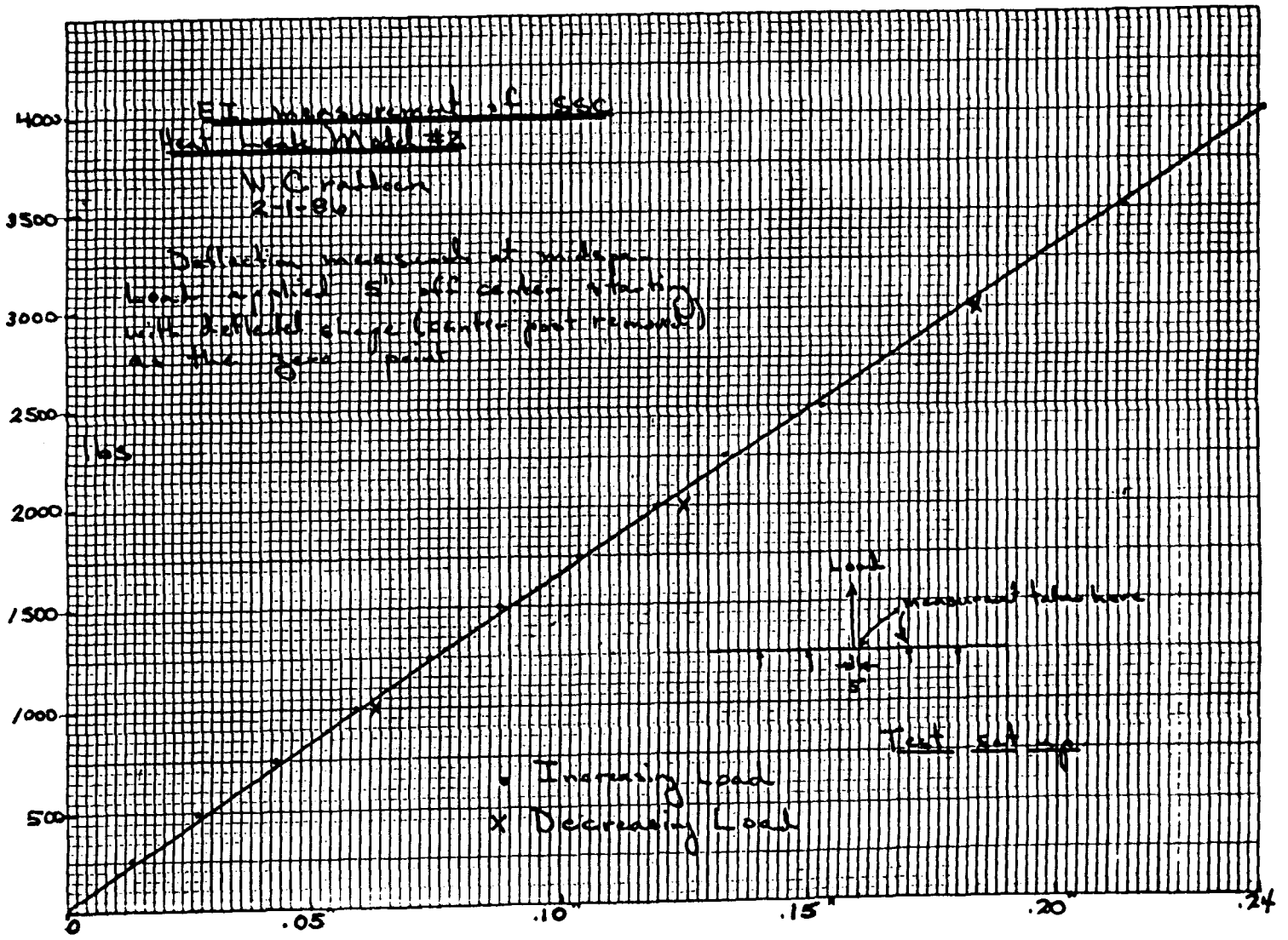

Fig. 2-2: Results of Cold Mass Stiffness Test Conducted by Fermilab. (Center support was removed and a 4000lb. vertical load applied 5 in. off center)

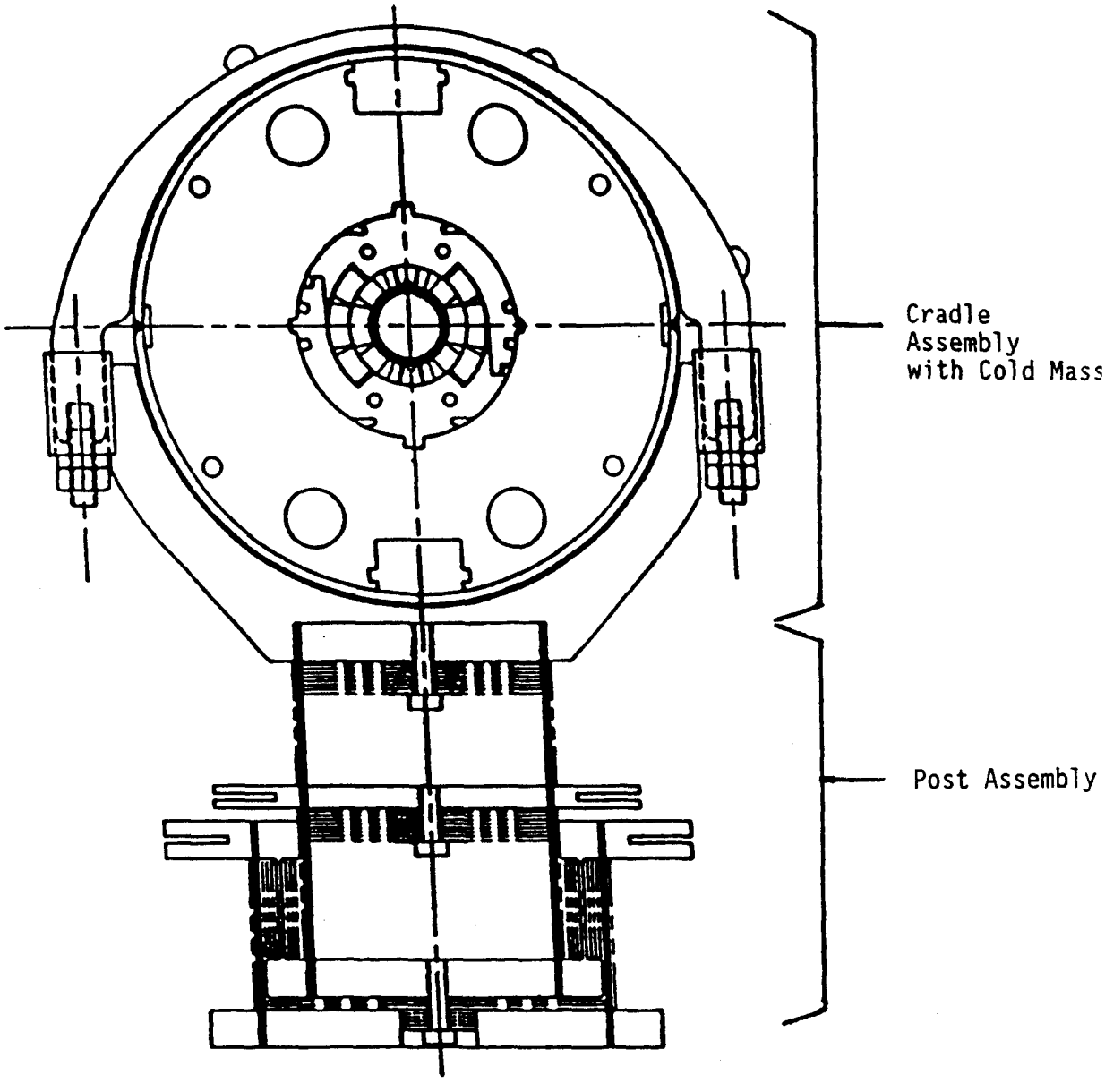

Fig. 2-3: Cold Mass Support Assembly

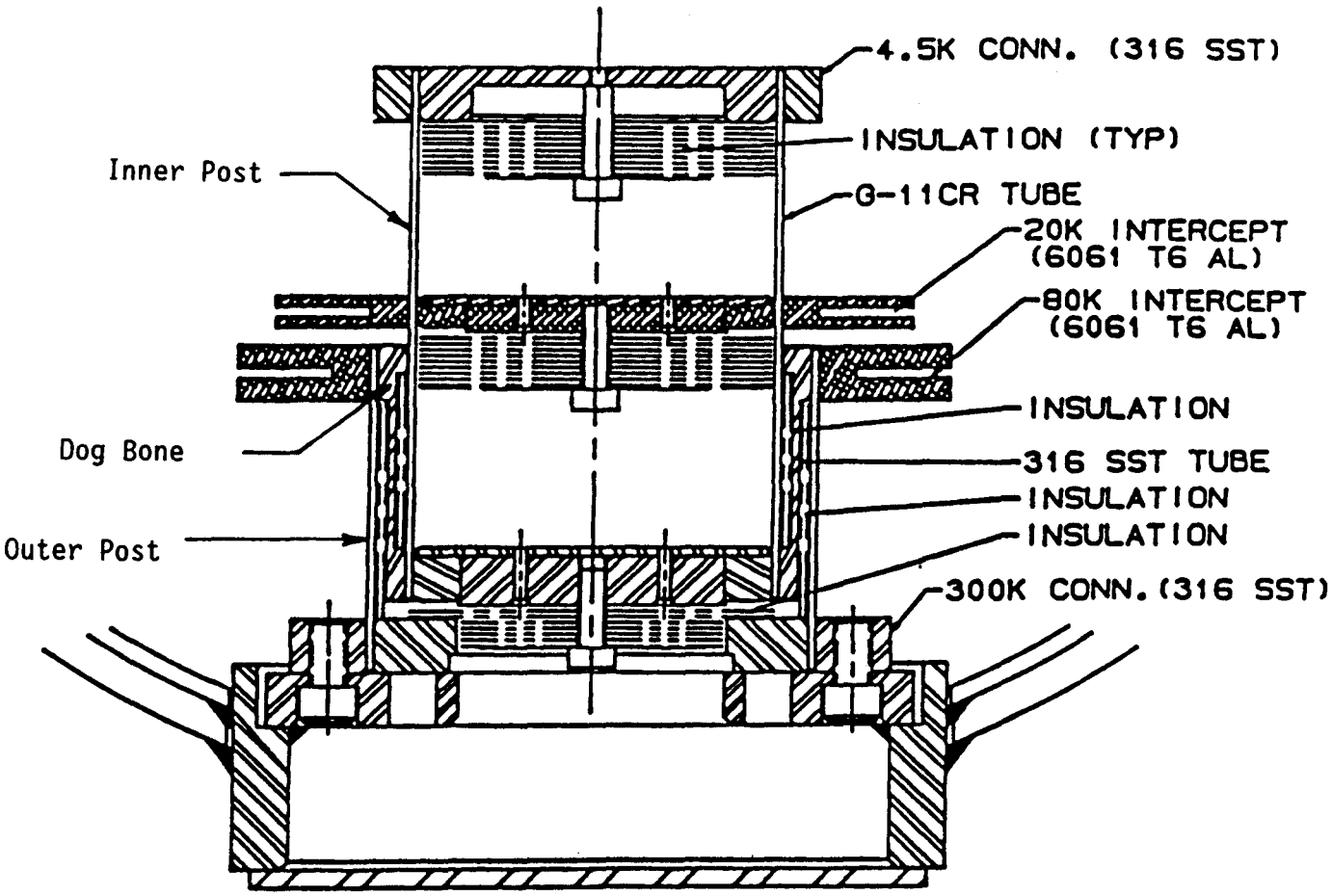

Fig. 2-4: Re-entrant Post Design

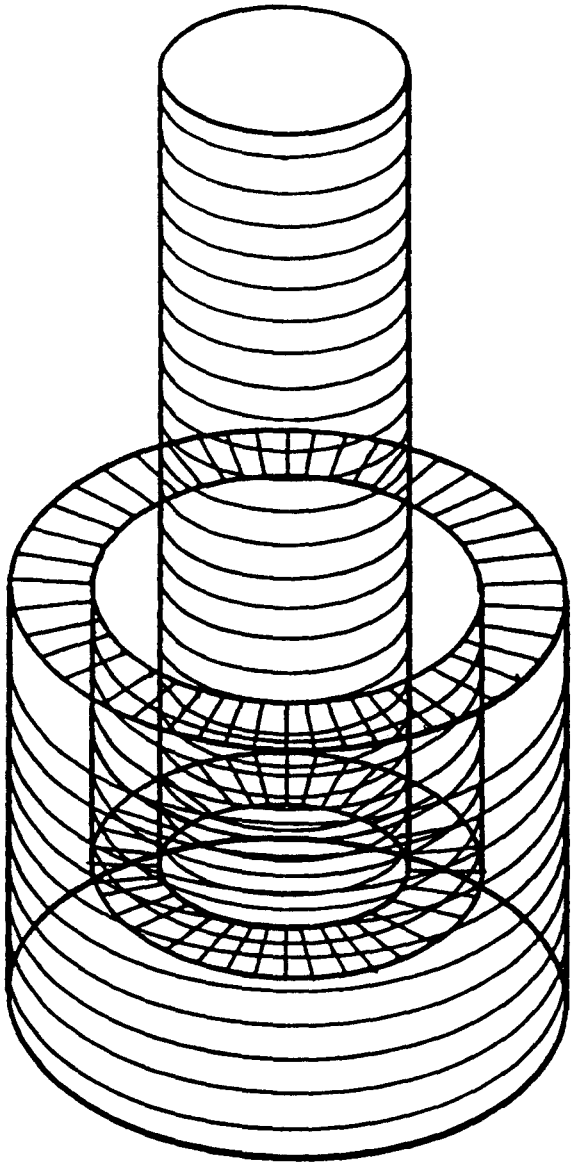

Fig. 2-5: Schematic of Support Post Finite Element Model

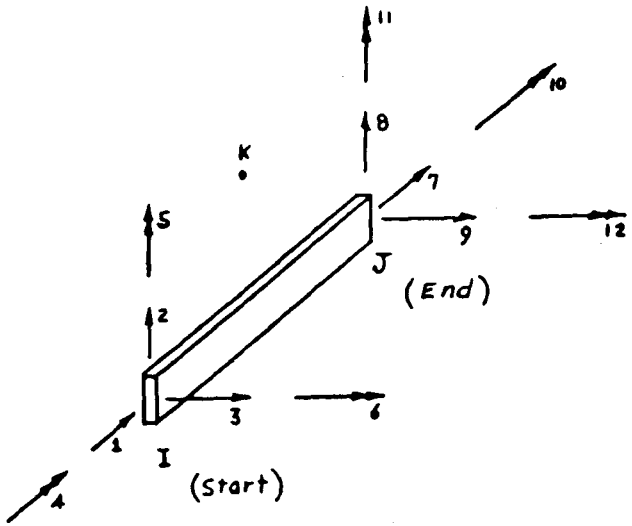

$$
\begin{bmatrix}
1590 & & & & & \\
 & 371 & & & & -1800 \\
 & & 371 & & 1800 & \\
 & & & 5260 & & \\
 & & 1800 & & 16200 & \\
 & -1800 & & & & 16200
\end{bmatrix}
$$

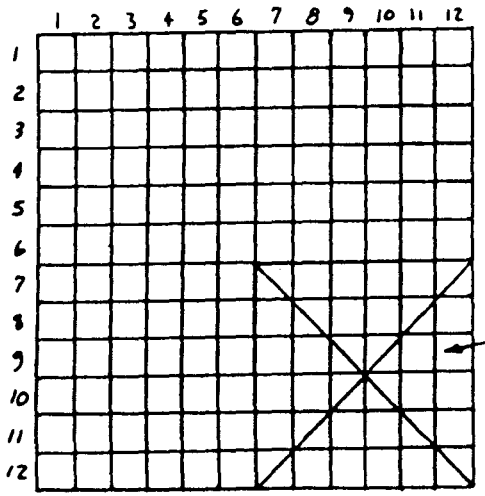

6x6 member end stiffness or member end flexibility matrix

Fig. 2-6: Stiffness Matrix for Re-entrant Post (Kips, in.)

EQE

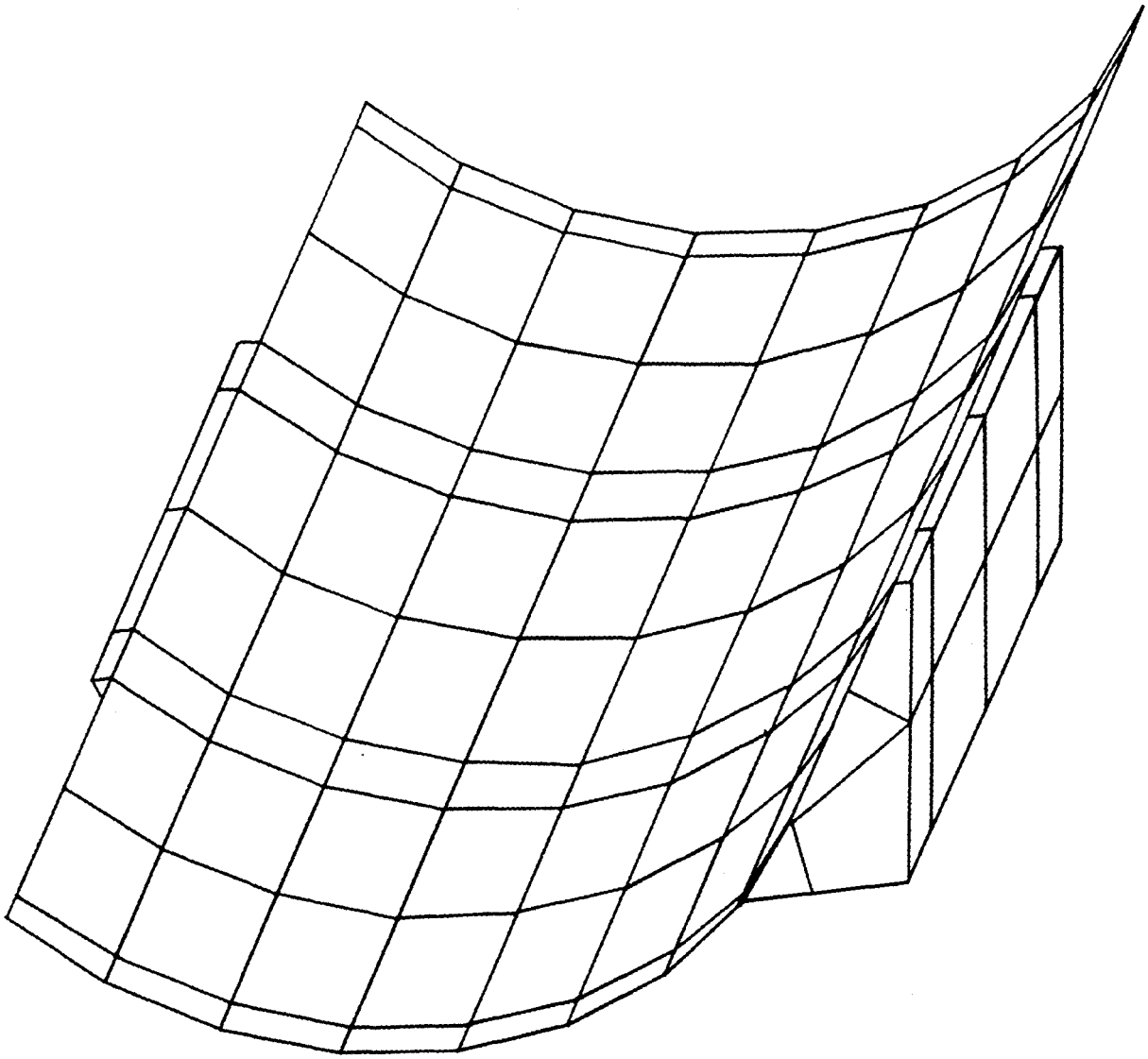

Fig. 2-7: Schematic of Center Cradle Finite Element Model

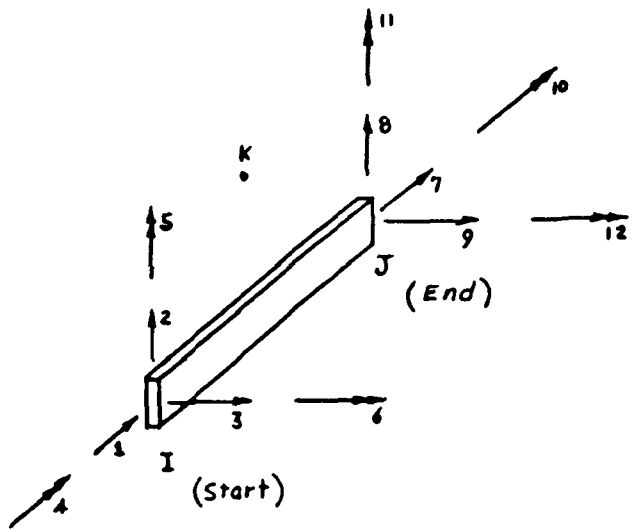

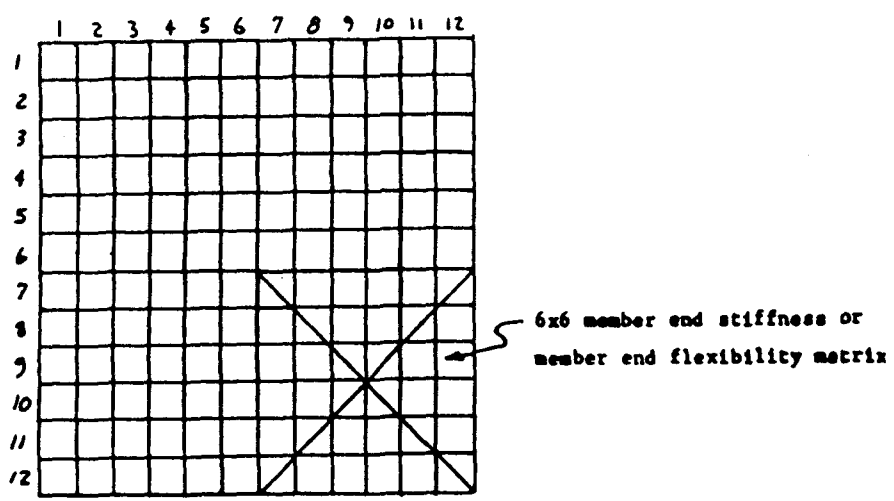

$$\begin{bmatrix} 111500 & & & & & \\ & 68240 & & & & -469100 \\ & & 82540 & & 556200 & \\ & & & 939300 & & \\ & & 556200 & & 41438000 & \\ & -469100 & & & & 3954000 \end{bmatrix}$$

Fig. 2-8: Stiffness Matrix for Center Cradle (Kips, in.)

EQE

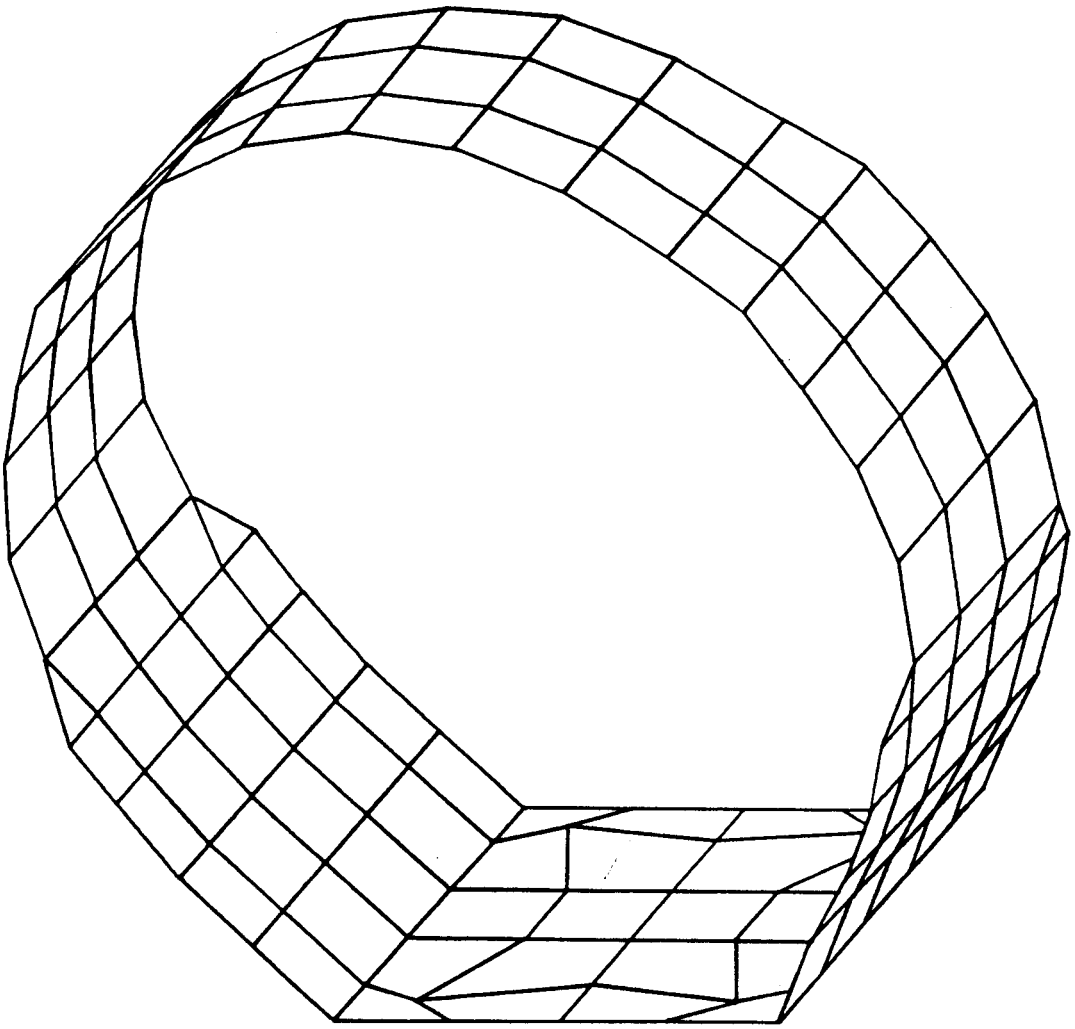

Fig. 2-9: Schematic of Outboard Cradle Finite Element Model

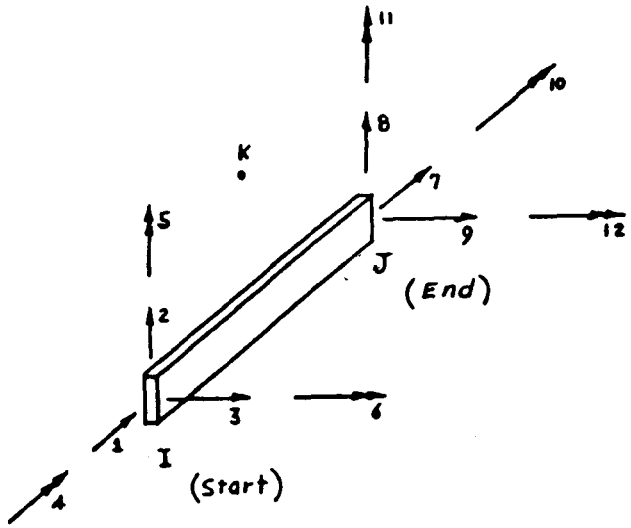

$$
\begin{bmatrix}
12300 & & & & & \\
 & 82900 & & & & -4159000 \\
 & & 116000 & & 803000 & \\
 & & & 14140000 & & \\
 & & 803000 & & 6790000 & \\
 & -4159000 & & & & 3080000
\end{bmatrix}
$$

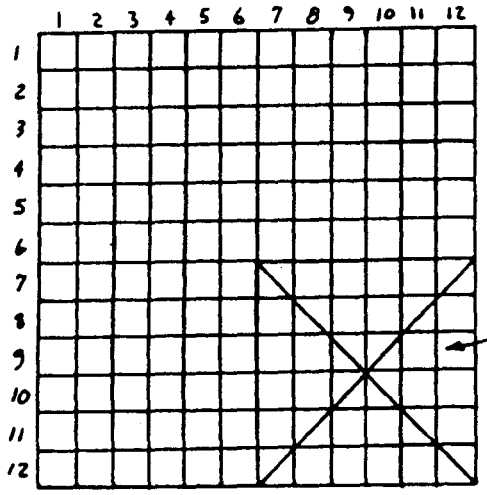

6x6 member end stiffness or member end flexibility matrix

Fig. 2-10: Stiffness Matrix for Outboard Cradle (Kips, in.)

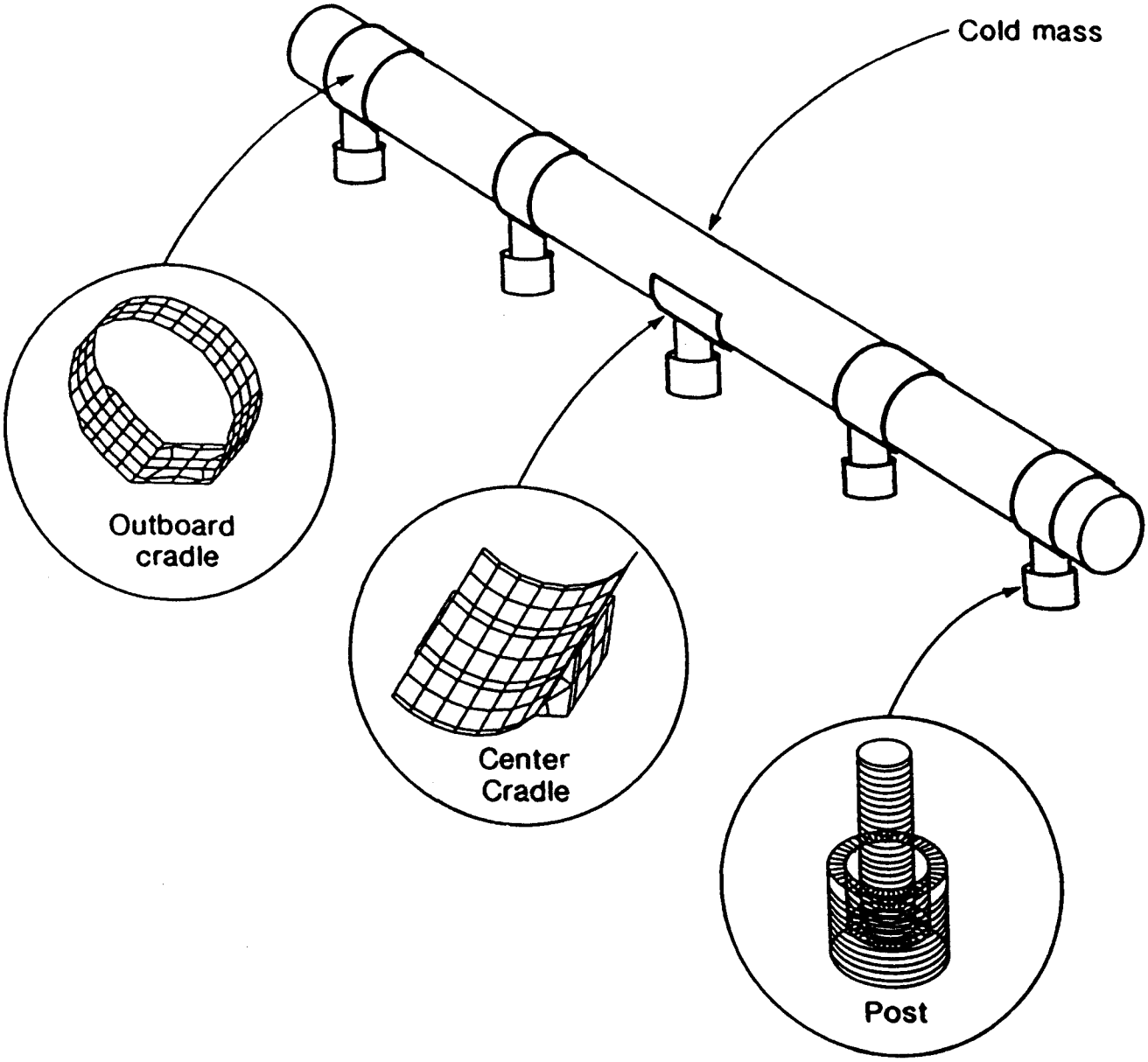

Fig. 2-11: Structural Components of Cold Mass Support System

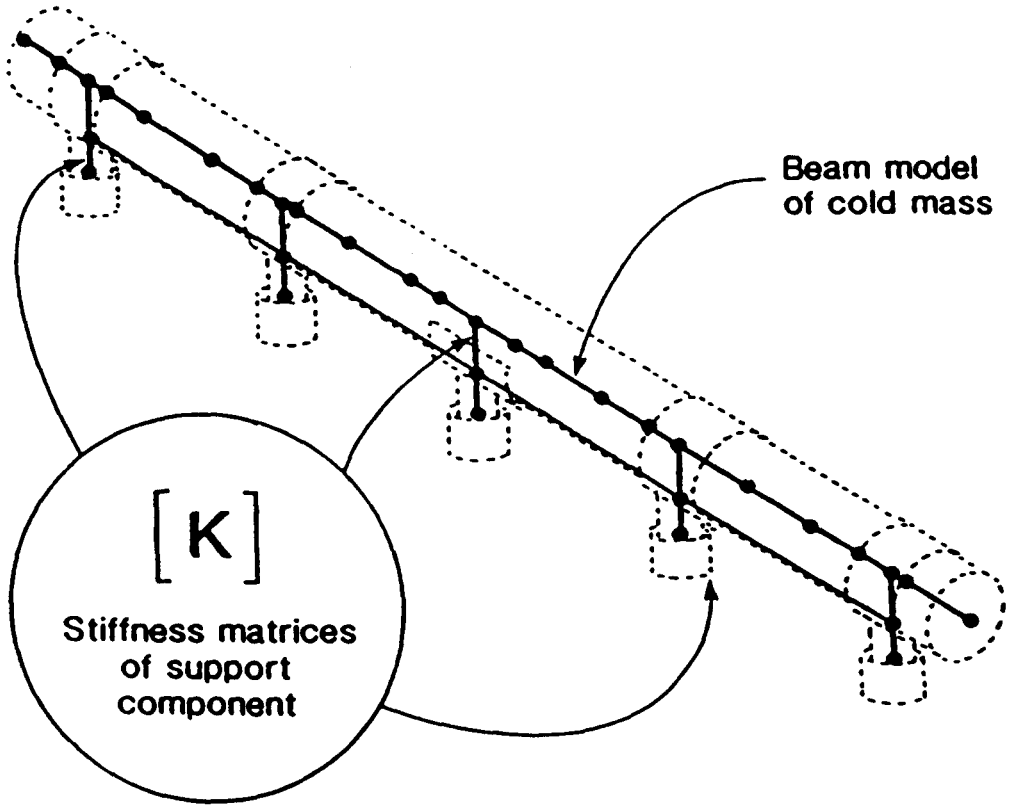

Fig. 2-12: Schematic of Substructure Approach

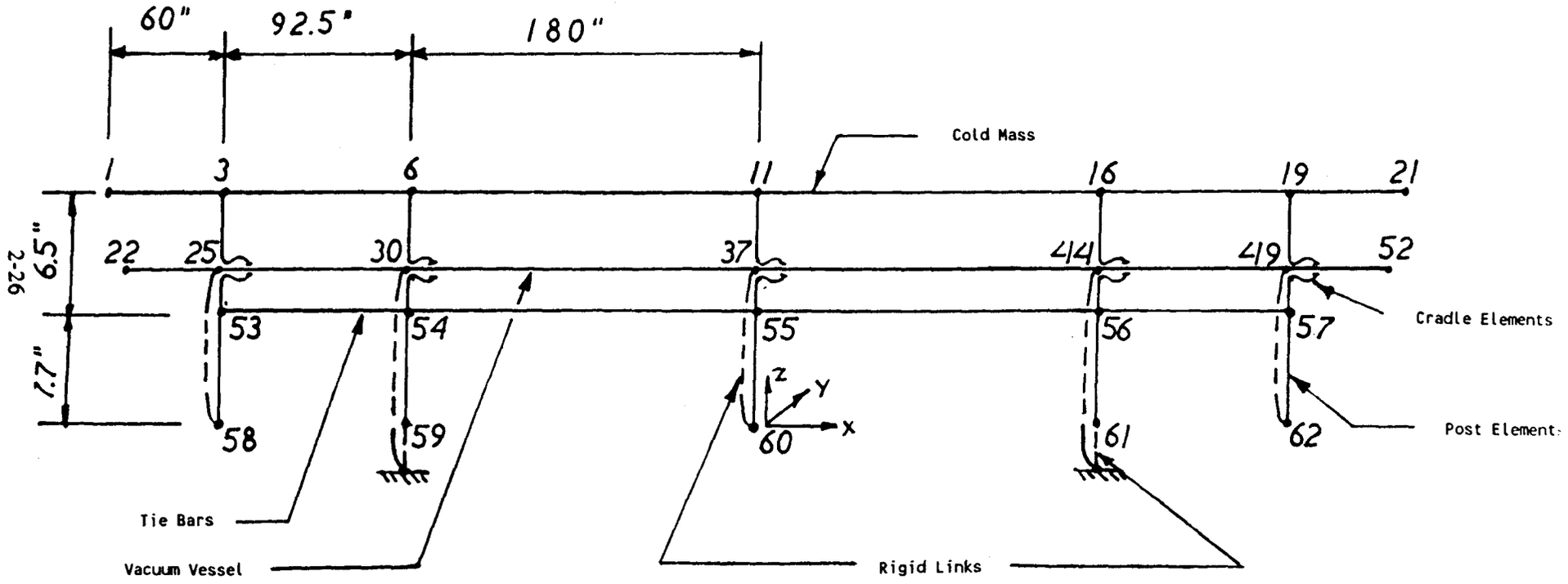

Fig. 2-13: Single Magnet Seismic Model

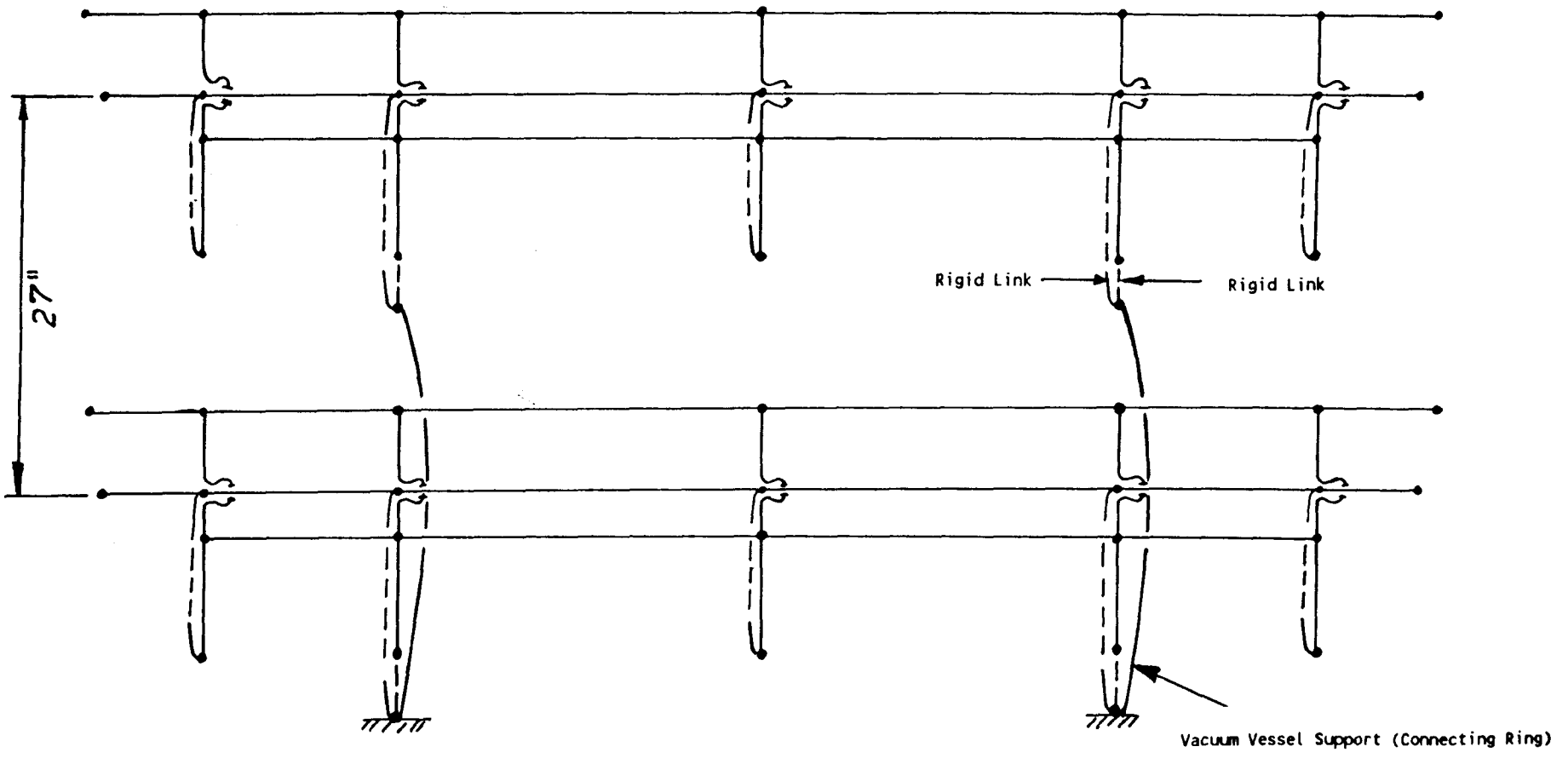

Fig. 2-14: Piggyback Seismic Model

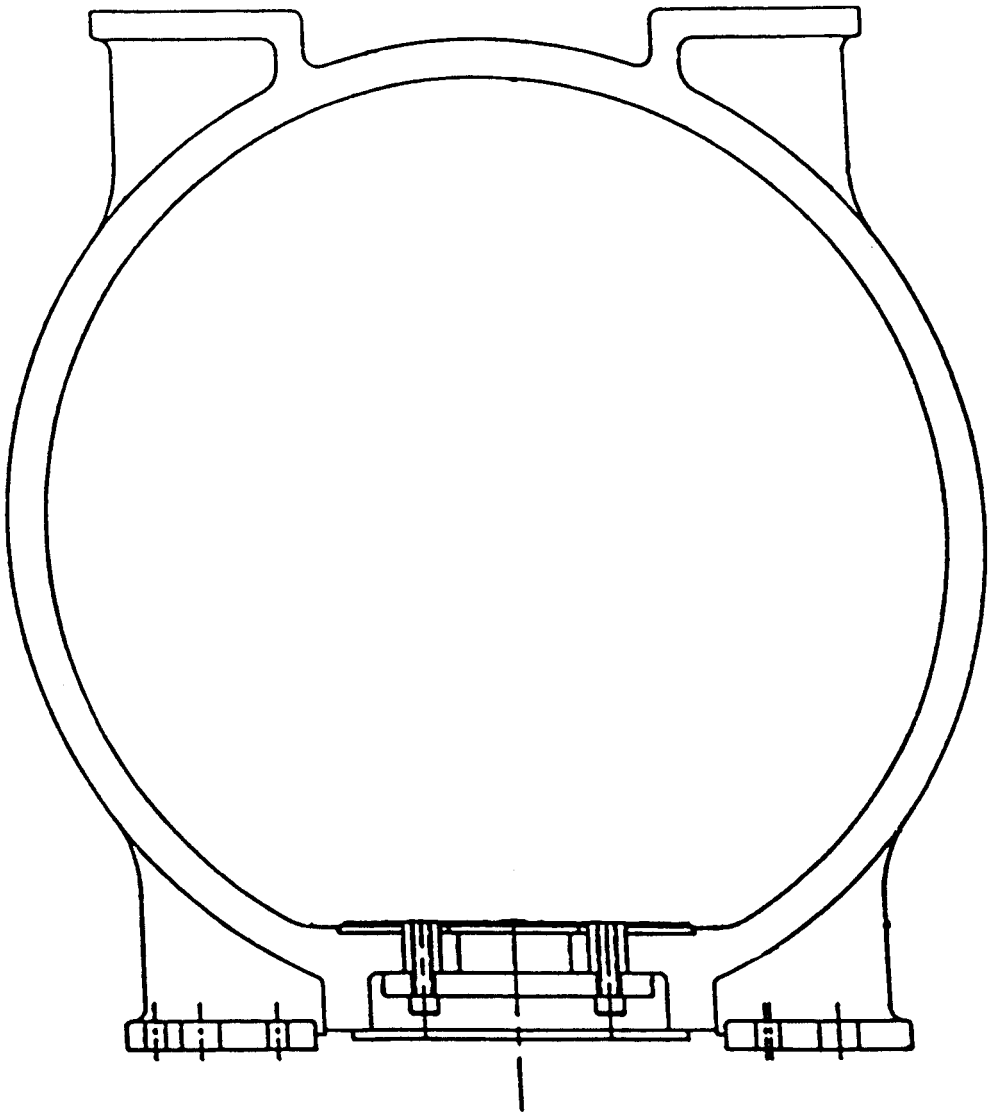

Fig. 2-15: Section View of Vacuum Vessel Support (Connecting Ring)

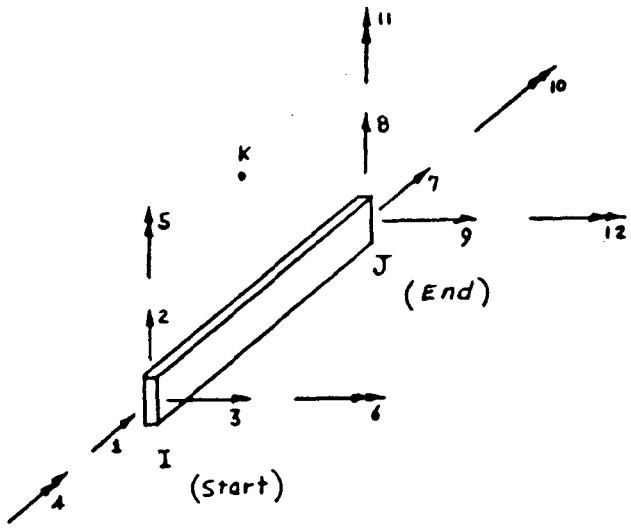

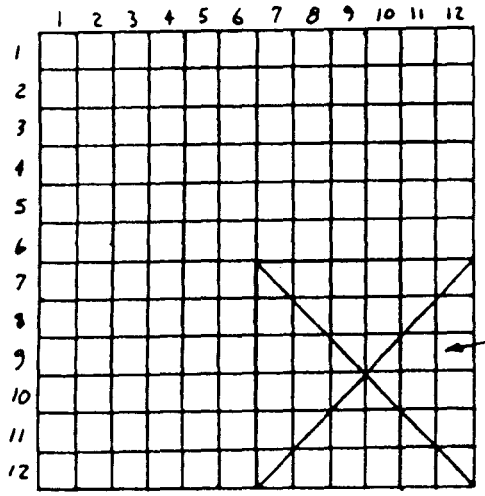

6x6 member end stiffness or member end flexibility matrix

$$\begin{bmatrix} 15416 & & & & & \\ & 19417 & & & & -24500 \\ & & 75 & & 12416 & \\ & & & 353360 & & \\ & & 12416 & & 208030 & \\ & -24500 & & & & 325150 \end{bmatrix}$$

Fig. 2-16: Stiffness Matrix for Support Ring (Kips, in.)

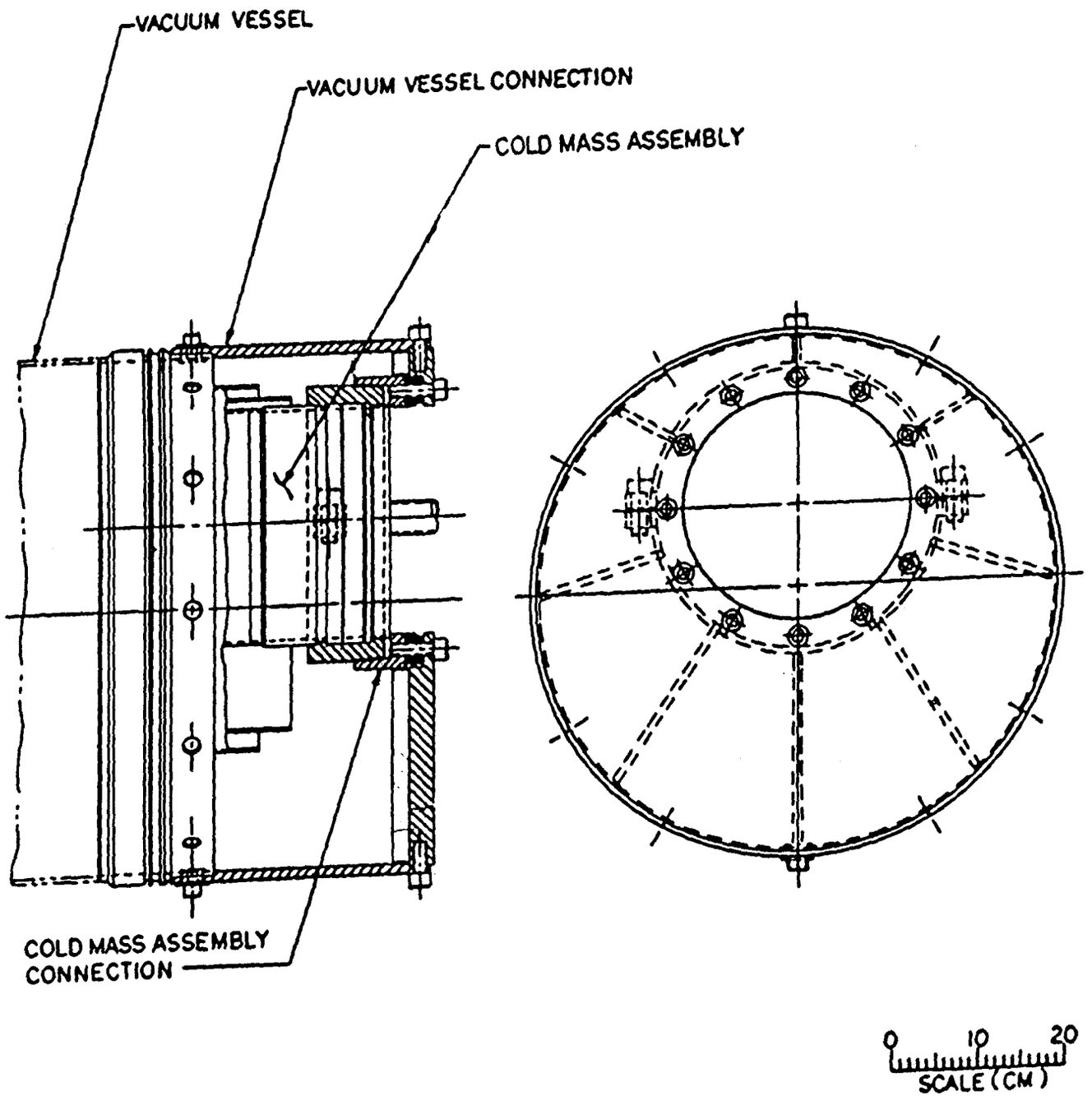

Fig. 2-17: External Axial Transportation Restraint

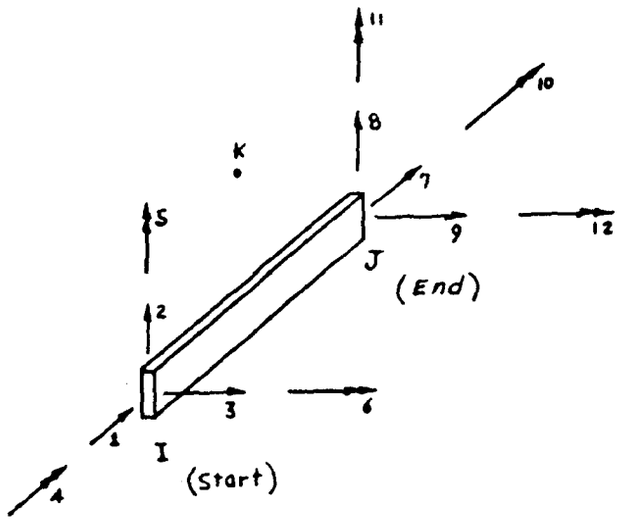

$$
\begin{bmatrix}
2140 & & & & & \\
 & 125000 & & & & 233000 \\
 & & 684100 & & -111000 & \\
 & & & \text{RIGID} & & \\
 & & -111000 & & 223000 & \\
 & 233000 & & & & 4641000
\end{bmatrix}
$$

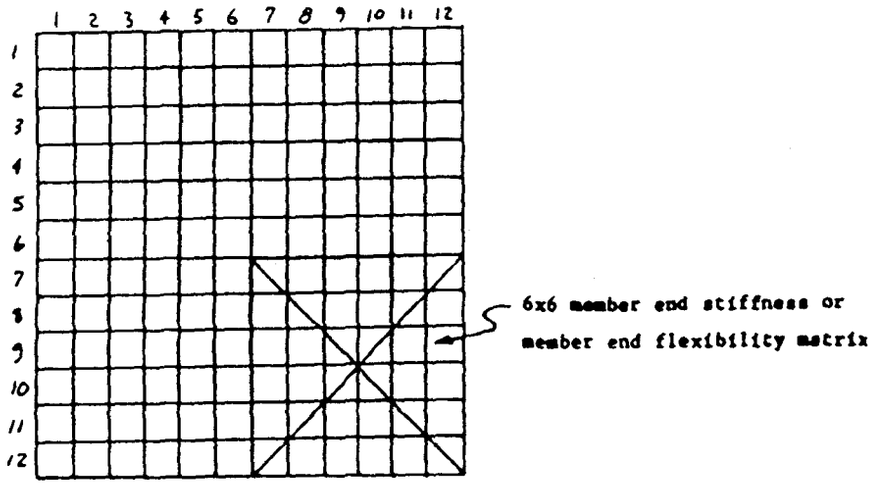

Fig. 2-18: Stiffness Matrix for Axial Transportation Restraint (Kips, in.)

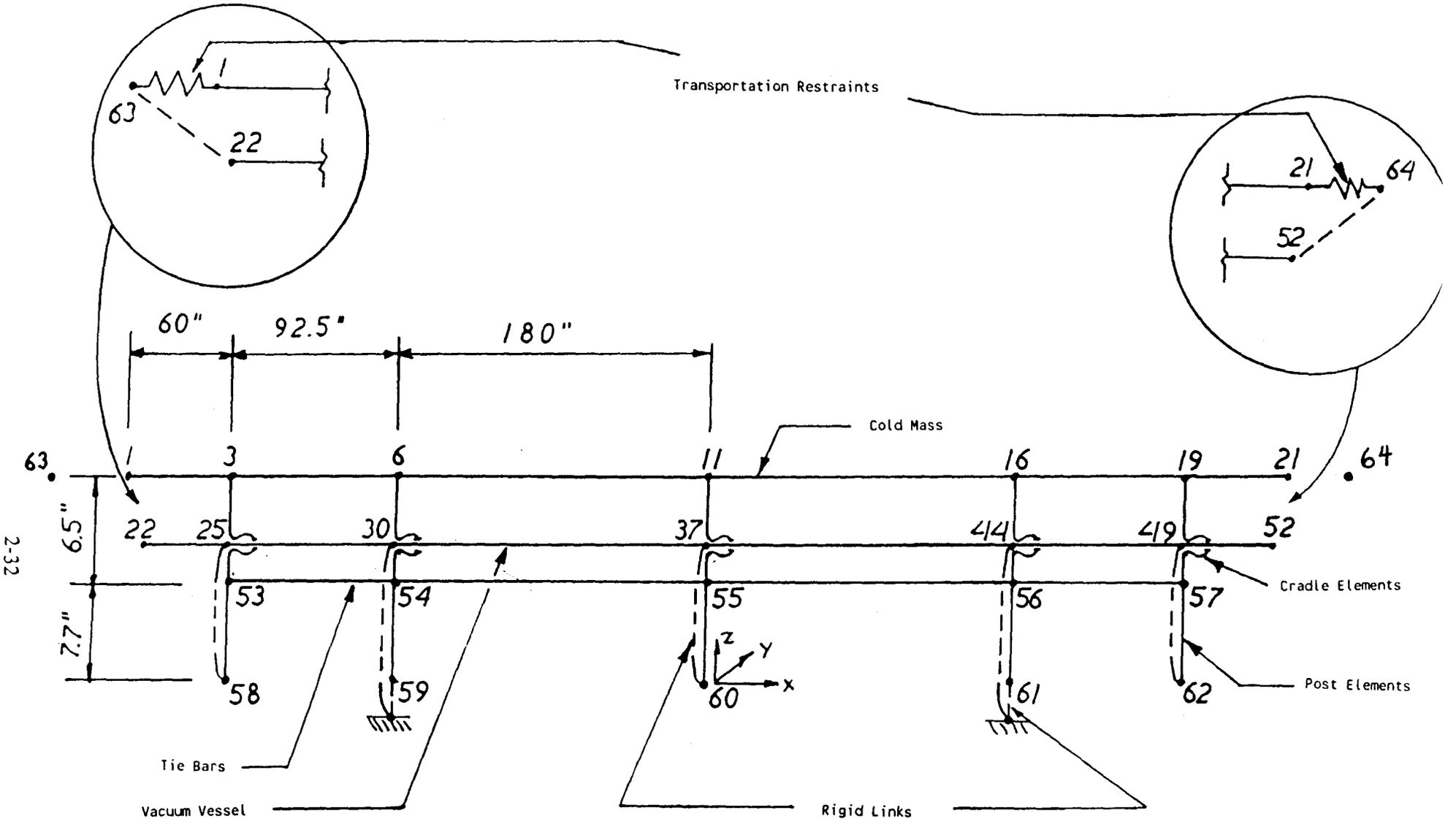

Fig. 2-19: Transportation Model

EQE

3.0 DYNAMIC RESPONSE ANALYSES AND RESULTS

3.1 DYNAMIC CHARACTERISTICS OF THE MAGNET SYSTEM MODELS

Three models were developed as described in Sec. 2 -- two seismic models (single and piggyback configurations) and the transportation model. Some general comments concerning their dynamic characteristics are in order before presenting the results of the dynamic analyses.

The single magnet system model can be viewed as a building block for the piggyback configuration and will be discussed first. For this model and the other two, response is uncoupled in the orthogonal directions of interest -- axial (along the cold mass), lateral, and vertical. Accordingly, significant modes and their relative mass participation are identified with one of these directions. Table 3.1 lists significant modes, their frequencies, mass participation, and direction for the single magnet system. The lowest frequency significant modes are associated with the lateral direction -- mode 1, 8.84 Hz, and 16.3% mass participation and mode 3, 10.16 Hz, and 56.2% mass participation. The two lowest frequency axial modes are modes 5 and 10 with frequencies and mass participation of 12.31 Hz, 27.1% and 17.56 Hz, 50.6%, respectively. Vertically, modes 6 and 8 are the lowest significant modes with frequencies and mass participation of 14.01 Hz, 21.3% and 14.71 Hz, 30.4% respectively. From the perspective of a seismic excitation, which can have amplified motion in the frequency range of 1 - 10 Hz, lateral direction response is most critical. Note, axially and vertically, the important modes have frequencies outside this amplified frequency range. The effect of the vacuum vessel on the frequencies of the magnet system can be assessed by performing an eigenvalue analysis of the cold mass and its support system without the vacuum vessel included. Table 3.2 lists significant modes, mass participation, and principal directions. This defines the basic behavior of the cold mass/support system. A comparison of Tables 3.1 and 3.2 shows the effect of the vacuum vessel -- a reduction in frequencies for lateral and vertical modes but little change in frequencies for axial modes. This comparison demonstrates the potential impact of stiffening the vacuum vessel on the dynamic characteristics of the single magnet system.

The piggyback configuration is the assembly of two single magnet systems. the lower magnet system behaves essentially the same as the single magnet system described above. The dynamic characteristics of the upper magnet system are affected by the support provided by the lower system. Table 3.3 lists significant modes, their frequencies, the lower or upper magnet system with which the mode is associated, the principal direction, and the mass participations as a percentage of the total mass and as a percentage of the upper magnet system mass, if appropriate. A comparison of Tables 3.1 and 3.3 shows the lower magnet system dynamic characteristics to be nearly identical to those of the single magnet system. The upper magnet system behavior, however, is significantly affected by it being supported by the lower magnet system. The fundamental lateral frequency of the upper magnet system is 5.92 Hz. This reduction in frequency has a significant effect on stresses induced in the support posts as discussed in subsequent sections. Note, however, that stiffening the lower vacuum vessel at the support locations will permit the upper magnet system dynamic characteristics to approach those of the lower system. The limiting excitation levels would then be nearly the same. For the axial and vertical directions, the upper magnet system dynamic characteristics are minimally affected.

The transportation model reflects the addition of an axial shipping restraint. Table 3.4 lists significant modes, their frequencies, mass participation, and direction. The overall behavior is simplified from the previous two cases. Also the axial shipping restraint increases the axial frequencies of the system.

3.2 RESPONSE TO SEISMIC EXCITATION

3.2.1 RG 1.60 Design Ground Response Spectra

The initial seismic design environment considered for both seismic models is specified by the horizontal and vertical design ground response spectra of the US NRC Regulatory Guide (RG) 1.60 anchored to a 0.3g peak ground acceleration (PGA). Three directional components of motion are specified -- two horizontal and one vertical. Figure 3-1 shows the horizontal design response spectrum for 5% damping.

These design ground response spectra are site-independent and appropriate for firm-to-stiff soil of a relatively uniform extent. They were developed from recorded motions on the surface of soil or rock and are targeted at approximately the mean - plus - one- standard - deviation exceedance level. In the context of these analyses, they may be interpreted in two ways. First, they represent a generic design criteria which will be compared with a site specific criteria when a particular site and depth in soil or rock is selected. Second, it represents a generic design criteria to which magnet systems stored on the surface of the soil prior to installation may be subjected.

The results presented in this section are summaries of stresses induced in the support post due to the earthquake excitation. The post stresses are focused on for a number of reasons. Namely, the highest stresses and the lowest allowables are indicative of the post. Seismic stresses in the cold mass are approximately 2 ksi or less. Seismic stresses in the tie bars are less than 2 ksi, and seismic stresses in the cradles are less than 9 ksi. The above mentioned components all have a significantly higher allowable stress than the maximum values of stress indicated.

Stresses in the support post were obtained by the substructuring process described previously, i.e., the detailed model of the post is subjected to the forces and moments determined from the dynamic response of the overall model; stress resultants and then stresses are calculated. A post-processor was written and used to combine membrane and bending stresses.

Tables 3.5, 3.6, and 3.7 present principal stresses at the most highly stressed areas of the center post for axial, lateral, and vertical earthquake motions. Note, these stresses are separated by earthquake direction which is appropriate for axial and lateral earthquake components because they represent maximum stresses which occur at different locations around the circumference. By inspection, combined stresses at other locations around the circumference are less. In all cases, the stresses due to the vertical earthquake should be combined with those due to lateral and axial earthquake components by the square-root-of-the-sum-of-the-squares (SRSS) rule. However, the stress values are extremely low and shown separately for display purposes. Elements 1 and 11 are in the outer cylinder with a minimum ultimate strength of 40,000 psi. Element 22 is in the stainless steel dog

bone. Elements 27 and 50 are in the inner cylinder with a minimum ultimate strength of 60,000 psi. Note, only the center post is presented -- the outer four posts are stressed less due to the axial earthquake component and approximately the same for lateral and vertical components.

Table 3.5 contains results for the single and piggyback models subject to the RG 1.60 design spectra assuming 5% damping and anchored to 0.3g PGA. This table also indicates allowable stresses which vary depending on location within the post. Note, however, these allowable stresses are for specified load combinations which are not included here. In general, the allowable stress listed in the tables is calculated as 33% of ultimate stress increased by 20% for seismic. They are presented here for information purposes only. Based on a combination of dead load and dynamic stresses and the given allowables in Table 3.5, though, the peak ground accelerations the single and piggyback magnet systems could withstand are 0.32g and 0.21g respectively. As indicated, axial and vertical stresses for both models are approximately the same. For the lateral direction, however, stresses in the support posts for the upper magnet system are about 1.6 times those of the lower magnet due to the reduced frequency of the lateral modes. The upper center post in the piggyback configuration is overstressed due to lateral excitations for RG 1.60 anchored to 0.3g PGA without considering any load combinations. Stresses due to axial excitation are actually slightly higher in the lower magnet system for the center post of the piggyback model which indicates a slight redistribution of axial load as a result of including the upper magnet. In the other two directions, though, the upper magnet dominates response behavior.

3.2.2 Site Specific Design Spectra Response

The RG 1.60 design spectra are broad-banded, meaning the time history records from which the spectra were derived are rich in frequency content, from 3-9 Hz. Site specific spectra are typically more narrow-band and reflect specific conditions at the site. For the following seismic analyses, a typical soft soil site, characterized by a shear wave velocity of 1000 ft/sec, was assumed. Earthquake motions recorded on soft soil are rich primarily in the lower frequency range whereas records on rock reflect a higher frequency content. Since the predominant

frequency range for both seismic models is greater than 6 Hz, assuming a soft soil site reduces the design spectral accelerations in this range.

In order to generate an appropriate design response spectra for a soft soil site, six actual earthquake time histories recorded at the surface of three soft soil sites were obtained (two horizontal components for each site)[6]. These were:

- El Centro (Imperial Valley) - May 18, 1940
  Components: S00^{o}E, S90^{o}W
- San Fernando (8244 Orion Blvd - 1st floor)
  February 9, 1971
  Components: N00^{o}W, S90^{o}W
- Ferndale (City Hall) - December 21, 1954
  Components: N44^{o}E, N46^{o}W

From these time histories, response spectra were generated as shown in Fig. 3-2. Mean and mean-plus-one-standard-deviation response spectra were generated for these six. The seismic analyses performed herein were for the mean-plus-one-standard-deviation response spectra following the philosophy of RG 1.60 and typical site specific evaluations. Figure 3-3 compares RG 1.60, the mean spectrum, and the mean-plus-one-standard-deviation spectrum. Note the spectral acceleration decrease in the higher frequency range compared to RG 1.60.

Table 3.6 presents results for the single and piggyback models subjected to this site specific spectrum at the ground surface in both horizontal directions and assuming the magnet configuration to be founded on the soil surface. Two-thirds of this spectrum was used for the vertical design spectrum. As before, post stresses are given at five locations within the center post according to coordinate direction. The beneficial effects of using a soft soil design spectrum are readily apparent from the single magnet results. Stresses in all three coordinate directions, especially lateral, decrease compared to the RG 1.60 case. Stresses due to lateral excitations still control the design. However, assuming design spectra appropriate for a soft soil site increases the peak ground acceleration which the single magnet can withstand to 0.44g at the surface based on the seismic and dead load combination and allowable stresses specified here.

For the piggyback model however, the allowable peak ground acceleration only increased to 0.25g, again being limited by stresses in the upper magnet support post induced by the lateral motion. To increase the seismic capability of the piggyback configuration, three options are readily identified. First, modify the support post design to permit higher allowable stresses or to reduce calculated seismic stresses. Second, increase the lateral stiffness of the vacuum vessel at the magnet system support locations which will increase the lateral frequency of the upper magnet system approaching that of the single or lower magnet system. Third, change the seismic design environment by using site specific design criteria and/or founding the system at depth in the soil.

Option 1 is not a preferred option since the support posts have been designed for all environmental conditions (especially temperature) and is satisfactory. In fact, option 1 is not necessary. A combination of options 2 and 3 will increase the seismic capability. A variation in siting conditions is investigated next by placing the system in a tunnel 30 feet below ground surface in the generic soft soil site.

The effect of founding the magnet system at depth is investigated next. A reduction in the design ground response spectra and its PGA is expected and consequently an increase in earthquake level which the magnet system can withstand. In general, the reduction in earthquake ground motion with depth in soil is expected. This phenomenon is observed in the field and is predicted by analytical techniques. To quantify the effect of placing the magnet system in a tunnel 30 feet beneath the ground surface, the following analyses were performed. A ten foot diameter tunnel was assumed to house the magnet system. The bottom of the tunnel was assumed to be 30 feet beneath the ground surface. Figure 3-4 shows a schematic of the tunnel. Two types of interaction theoretically occur between the tunnel and the surrounding soil during an earthquake -- kinematic interaction and inertial interaction. Kinematic interaction is basically the wave scattering and effective averaging of the motion. Inertial interaction is the dynamic interaction of the soil and structure and is significant for large massive structures. For the present case, only kinematic interaction is of significance. To account for kinematic interaction, a model of the tunnel and surrounding soil was developed and analyzed using the computer program FLUSH [7]. The tunnel was modeled as a rigid massless inclusion in a uniform half-space of shear wave

velocity of 1000 ft/sec. The tunnel behaves rigidly compared to the soil. The representation was massless to obtain the significant wave scattering effects whereas inertial interaction effects would be minimal for this case. The FLUSH finite-element mesh is shown in Fig. 3-4. The analyses proceeded by defining the control point on the ground free surface and the control motion as the six recorded acceleration time histories described above. All six were scaled to 0.3g PGA. Note, no strain dependent soil properties were assumed -- soil properties remained fixed. Six analyses were performed and acceleration time histories for each analysis were generated at several points on the tunnel/soil interface. Response spectra were generated and horizontal motions compared. The tunnel was observed to be excited laterally as a rigid body with negligible rotation. Hence, acceleration time histories from each of the six analyses were calculated at the bottom of the tunnel (node 64, Fig. 3-4) and considered appropriate for evaluation of the magnet system. Mean and mean-plus-one-standard-deviation spectra were calculated from these six and shown in Figs. 3-5 and 3-6. The mean-plus-one-standard-deviation response spectrum became the input to the evaluation of the magnet system at depth. This follows the RG 1.60 philosophy discussed previously. Note, in the other horizontal direction, the motions on the tunnel would be expected to differ somewhat due to the difference in geometry. However, since the primary calculated effect is a reduction in translations with negligible induced rotation, assuming the same design spectrum in both horizontal directions is a reasonable approximation. The vertical design spectrum was assumed to be two-thirds of the horizontal. This is clearly a rough approximation which will require further evaluation in future stages. This is adequate currently because vertical frequencies are relatively high and vertical response is far from governing.

Figure 3-7 shows an overplot of the three design response spectra considered here. The variation in amplitude and frequency content is clearly shown.

Table 3.7 presents the results from response spectrum analyses of the single and piggyback magnet systems. The single magnet under these assumed soil and foundation conditions can withstand an earthquake of 0.64g peak ground acceleration on the ground surface -- a 2.5 fold increase over the RG 1.60 case discussed previously. The piggyback model, however, can only accommodate an earthquake with peak ground acceleration on the ground surface of 0.37g.

3.3 RESPONSE TO TRANSPORTATION LOADING

The transportation design criteria specified for the SSC accounts for those loads anticipated during handling and transit of the cryostat system from place of fabrication to place of installation. The response of the cryostat assembly to the kinds of impulsive loadings defined by the transportation criteria is a function of the dynamic characteristics of the systems and the amplitude, shape, and configuration of the applied pulse. However, neither the shape nor the duration of the pulse is specified in the criteria; only the magnitude of the loading: 1.5g axial, 1.0g lateral, and 2.0g vertical. For this study, a range of loading durations depending on direction was considered as indicated in Fig. 3-8. The shape of the loading pulse was assumed to be a half-sine pulse with a period-dependent response spectrum.

A conventional response spectrum analysis was not possible since the design spectrum is based on an unspecified pulse duration, however a critical maximum response spectrum analysis was performed to yield the highest expected post stresses. Since the transportation model's response is governed by two significant modes per direction, a maximum spectrum had to be determined for each coordinate direction. In each case, the PGA of the spectrum was assumed 1g and results were scaled by 1.5 in the axial direction and 2.0 in the vertical direction to be consistent with the design criteria. Since the peak spectral accelerations vary according to period and pulse duration (whose range was determined), a single pulse duration was chosen such that the peak spectral value occurred at the more significant of the two known periods for that direction. In this way, the maximum dynamic amplification will occur at the period whose mode shape has the most mass participating in it. The spectral acceleration is then defined for the secondary mode in that direction because the duration at which the maximum occurs has already been determined. Of course, the duration chosen always remained within the bound of durations determined for the transportation loading. This process yielded three different design spectra, one for each direction. Figures 3-9, 3-10, and 3-11 show the axial, lateral, and vertical (respectively) half-sine pulse response spectra used in this analysis.

Table 3.8 presents results of this analysis for the transportation (single) model only. Allowable stresses are listed also based on slightly different criteria than for seismic analysis (20% lower). Shown are the dead load and pulse excitation stresses separately in each direction. For the transportation model, post stresses due to vertical excitation become excessive in addition to the very large stresses due to lateral shaking. The allowable stresses listed are for different loading combinations and not only for the pulse loading. This indicates that the posts will actually be more highly stressed than Table 3.8 suggests when load combinations are considered. Therefore the transportation criteria appear to govern the design of the SSC support configuration.

Table 3.1

CHARACTERISTIC MODES OF THE SINGLE MAGNET SEISMIC MODEL

Mode	Frequency (Hz)	Modal Mass (%)	Principal Direction
1	8.84	16.3	Lateral
3	10.16	56.2	Lateral
5	12.31	27.1	Axial
6	14.01	21.3	Vertical
8	14.71	30.4	Vertical
9	16.16	9.7	Lateral
10	17.56	50.6	Axial
13	27.70	15.0	Vertical
15	32.15	12.2	Vertical

Table 3.2

CHARACTERISTIC MODES OF THE COLD MASS/SUPPORT SYSTEM

Mode	Frequency (Hz)	Modal Mass (%)	Principal Direction
1	9.66	29.4	Lateral
3	11.26	55.8	Lateral
5	12.35	33.4	Axial
6	16.73	12.2	Lateral
7	17.18	28.0	Vertical
8	17.40	42.1	Axial
10	18.57	23.1	Axial
11	19.56	12.4	Vertical

Table 3.3

CHARACTERISTIC MODES OF THE PIGGYBACK CONFIGURATION
(U = UPPER MAGNET, L = LOWER MAGNET)

Mode	Frequency (Hz)	Modal Mass (%of Total)	Modal Mass (%of Upper)	Principal Direction
1	5.92	47.9	95.8	Lateral - U
4	8.84	8.0		Lateral - L
9	10.16	28.3		Lateral - L
11	12.17	14.2	28.4	Axial - U
12	12.31	13.5		Axial - L
13	12.84	29.3	58.6	Vertical - U
14	14.00	10.1		Vertical - L
17	14.69	15.7		Vertical - L
18	16.16	4.8		Lateral - L
20	16.23	22.3	44.6	Axial - U
21	17.59	25.3		Axial - L
26	25.88	13.4	26.8	Vertical - U
27	27.69	7.5		Vertical - L

Table 3.4

CHARACTERISTIC MODES OF THE TRANSPORTATION MODEL

Mode	Frequency (Hz)	Modal Mass (%)	Principal Direction
2	10.45	54.7	Lateral
4	14.87	38.5	Vertical
5	16.85	13.4	Lateral
10	37.71	59.5	Axial
12	43.10	14.2	Axial
13	46.46	22.2	Vertical

Table 3.5

SUPPORT POST MAXIMUM COMBINED MEMBRANE AND BENDING STRESSES

SEISMIC EXCITATION, RG 1.60 DESIGN SPECTRA ANCHORED TO 0.3G PGA(5% DAMPING)

Excitation Direction	Element Number	Static D. L. Stress (Ksi) (Single and Piggyback)	Maximum Stress (Ksi) Single Model	Maximum Stress (Ksi) Piggyback Model	Allowable Stress* (Ksi)
Axial	1	-2.38	-3.92	-3.88 (L)	16.0
Lateral	1	-2.38	12.45	20.45	16.0
Vertical	1	-2.38	-1.19	-1.36	16.0
Axial	11	-2.03	1.15	1.18 (L)	16.0
Lateral	11	-2.03	7.71	12.66	16.0
Vertical	11	-2.03	-1.02	-1.16	16.0
Axial	22	2.92	3.00	2.94 (L)	28.0
Lateral	22	2.92	-15.49	-25.44	28.0
Vertical	22	2.92	1.47	1.67	28.0
Axial	27	-2.64	-3.36	-3.30 (L)	24.0
Lateral	27	-2.64	17.37	28.53	24.0
Vertical	27	-2.64	-1.32	-1.51	24.0
Axial	50	-2.66	8.35	8.44 (L)	24.0
Lateral	50	-2.66	8.20	13.50	24.0
Vertical	50	-2.66	-1.34	-1.52	24.0

*Based on Ref. 1. These allowable values are not for seismic only and are shown here for information only.

(L) = Lower Magnet

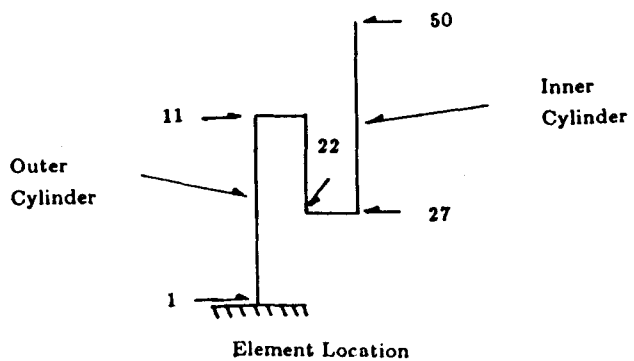

Table 3.6

SUPPORT POST MAXIMUM COMBINED MEMBRANE AND BENDING STRESSES
SEISMIC EXCITATION, SOFT SOIL DESIGN SPECTRA ANCHORED TO 0.3G PGA, SURFACE FOUNDED (5% DAMPING)

Excitation Direction	Element Number	Static D. L. Stress (Ksi) (Single and Piggyback)	Maximum Stress (Ksi) Single Model	Maximum Stress (Ksi) Piggyback Model	Allowable Stress* (Ksi)
Axial	1	-2.38	-2.88	-2.85 (L)	16.0
Lateral	1	-2.38	8.52	16.81	16.0
Vertical	1	-2.38	-0.58	-0.66	16.0
Axial	11	-2.03	0.87	0.90 (L)	16.0
Lateral	11	-2.03	5.27	10.42	16.0
Vertical	11	-2.03	-0.50	-0.56	16.0
Axial	22	2.92	2.18	2.14 (L)	28.0
Lateral	22	2.92	-10.59	-20.92	28.0
Vertical	22	2.92	0.72	0.81	28.0
Axial	27	-2.64	-2.45	-2.40 (L)	24.0
Lateral	27	-2.64	11.88	23.46	24.0
Vertical	27	-2.64	-0.65	-0.73	24.0
Axial	50	-2.66	6.27	6.34 (L)	24.0
Lateral	50	-2.66	5.61	11.10	24.0
Vertical	50	-2.66	-0.65	-0.74	24.0

*Based on Ref. 1. These allowable values are not for seismic only and are shown here for information only.
(L) = Lower Magnet

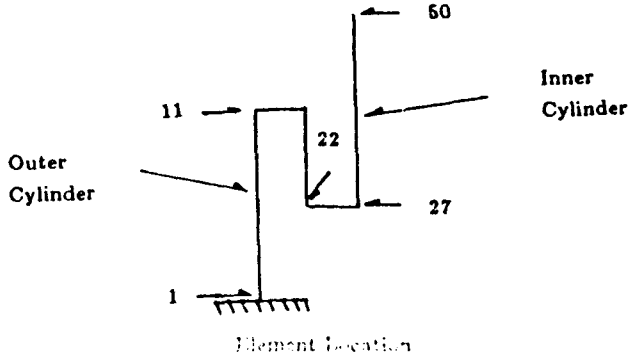

Table 3.7

SUPPORT POST MAXIMUM COMBINED MEMBRANE AND BENDING STRESSES

SEISMIC EXCITATION, SOFT SOIL DESIGN SPECTRA ANCHORED TO 0.3G PGA, FOUNDED AT -30 FT. (5% DAMPING)

Excitation Direction	Element Number	Static D. L. Stress (Ksi) (Single and Piggyback)	Maximum Stress (Ksi) Single Model	Maximum Stress (Ksi) Piggyback Model	Allowable Stress* (Ksi)
Axial	1	-2.38	-2.21	-2.19 (L)	16.0
Lateral	1	-2.38	5.04	10.55	16.0
Vertical	1	-2.38	-0.42	-0.47	16.0
Axial	11	-2.03	0.73	0.75 (L)	16.0
Lateral	11	-2.03	3.12	6.54	16.0
Vertical	11	-2.03	-0.36	-0.41	16.0
Axial	22	2.92	1.63	1.60 (L)	28.0
Lateral	22	2.92	-6.27	-13.13	28.0
Vertical	22	2.92	0.52	0.58	28.0
Axial	27	-2.64	-1.83	-1.79 (L)	24.0
Lateral	27	-2.64	7.03	14.71	24.0
Vertical	27	-2.64	-0.47	-0.53	24.0
Axial	50	-2.66	5.06	5.12 (L)	24.0
Lateral	50	-2.66	3.32	6.97	24.0
Vertical	50	-2.66	-0.47	-0.53	24.0
Input PGA (at Surface)		0.3g	0.3g		
Input PGA (at -30 ft.)		0.27g	0.27g		

*Based on Ref. 1. These allowable values are <u>not</u> for seismic only and are shown here for information only.

(L) = Lower Magnet

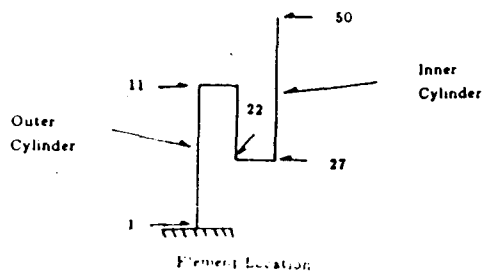

Table 3.8

SUPPORT POST MAXIMUM COMBINED MEMBRANE AND BENDING STRESSES

TRANSPORTATION EXCITATION, HALF-SINE PULSE DESIGN SPECTRA (5% DAMPING)

Excitation Direction	Element Number	Static D. L. Stress (Ksi) (Single and Piggyback)	Maximum Stress (Ksi) (by direction)	Allowable Stress* (Ksi)
Axial	1	-2.38	-4.92	13.3
Lateral	1	-2.38	23.97	13.3
Vertical	1	-2.38	-8.32	13.3
Axial	11	-2.03	1.05	13.3
Lateral	11	-2.03	11.03	13.3
Vertical	11	-2.03	-7.10	13.3
Axial	22	2.92	4.05	23.3
Lateral	22	2.92	-26.55	23.3
Vertical	22	2.92	10.22	23.3
Axial	27	-2.64	-4.55	20.0
Lateral	27	-2.64	29.78	20.0
Vertical	27	-2.64	-9.22	20.0
Axial	50	-2.66	8.87	20.0
Lateral	50	-2.66	-3.56	20.0
Vertical	50	-2.66	-9.30	20.0

*Based on Ref. 1. These allowable values are not for transportation loads only and are shown here for information only.

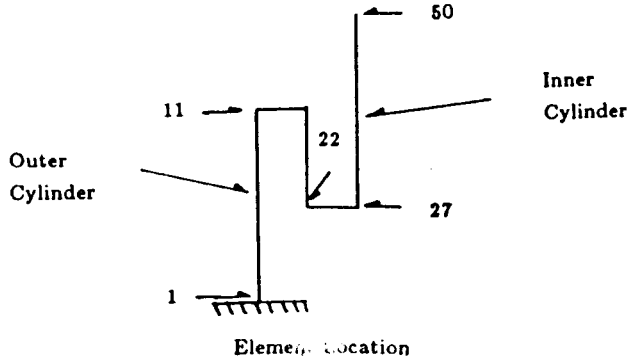

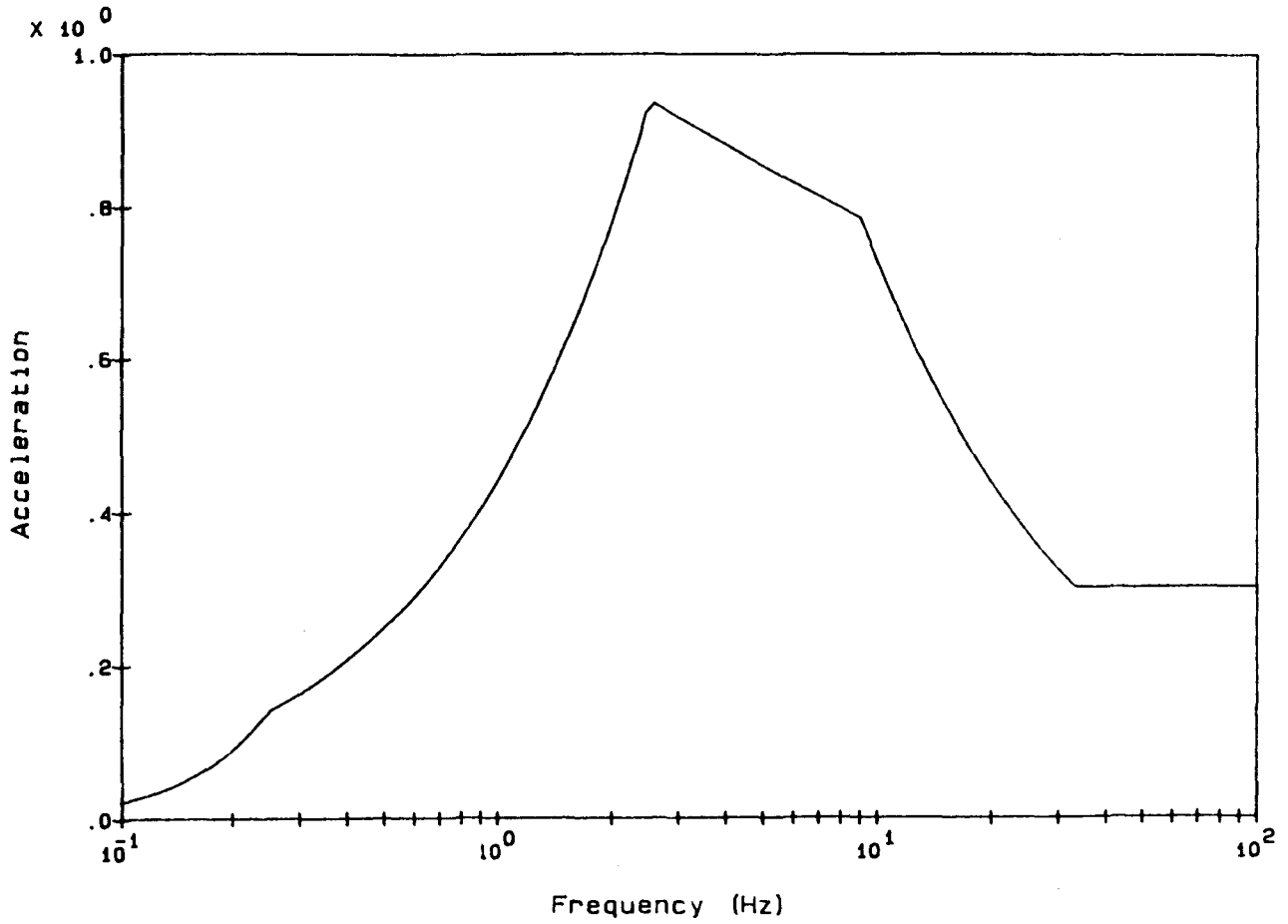

Notes:

horizontal spectrum

damping = 5%

accelerations in (g)

Fig. 3-1: Design Response Spectrum RG 1.60 Scaled to 0.3g

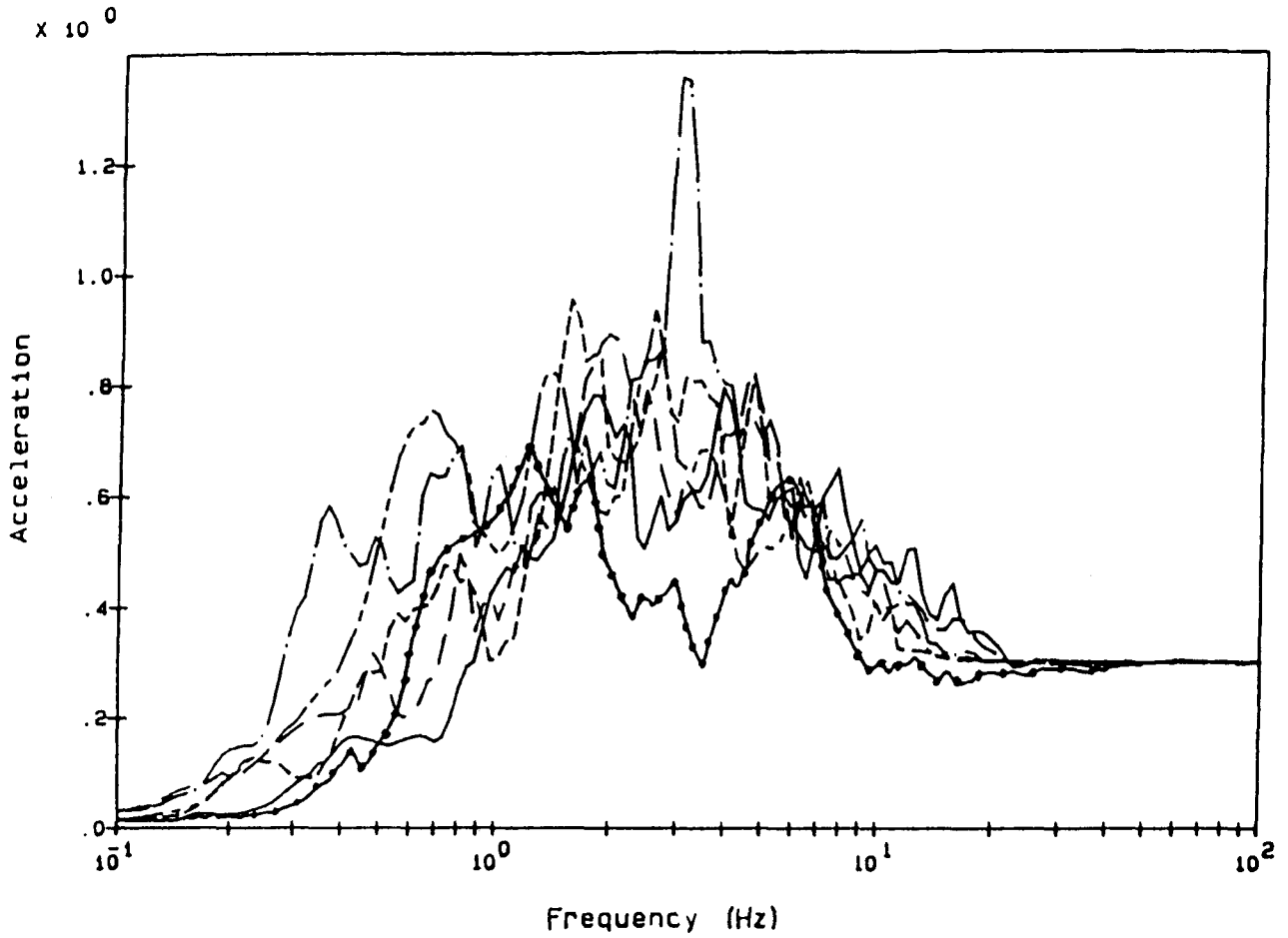

Legend:

El Centro	s00e	————
El Centro	s90w	— — — — .
San Fernando	n00w	- - - - - - - - .
San Fernando	s90w	——— . ——— ..
Ferndale	n44e	—— - - —— - - .
Ferndale	n46w	•—•—•—•—•—•

Notes:

damping = 5%
accelerations in (g)
scaled to 0.3 g

Fig. 3-2: Site Specific Response Spectra at Surface (Six Components)

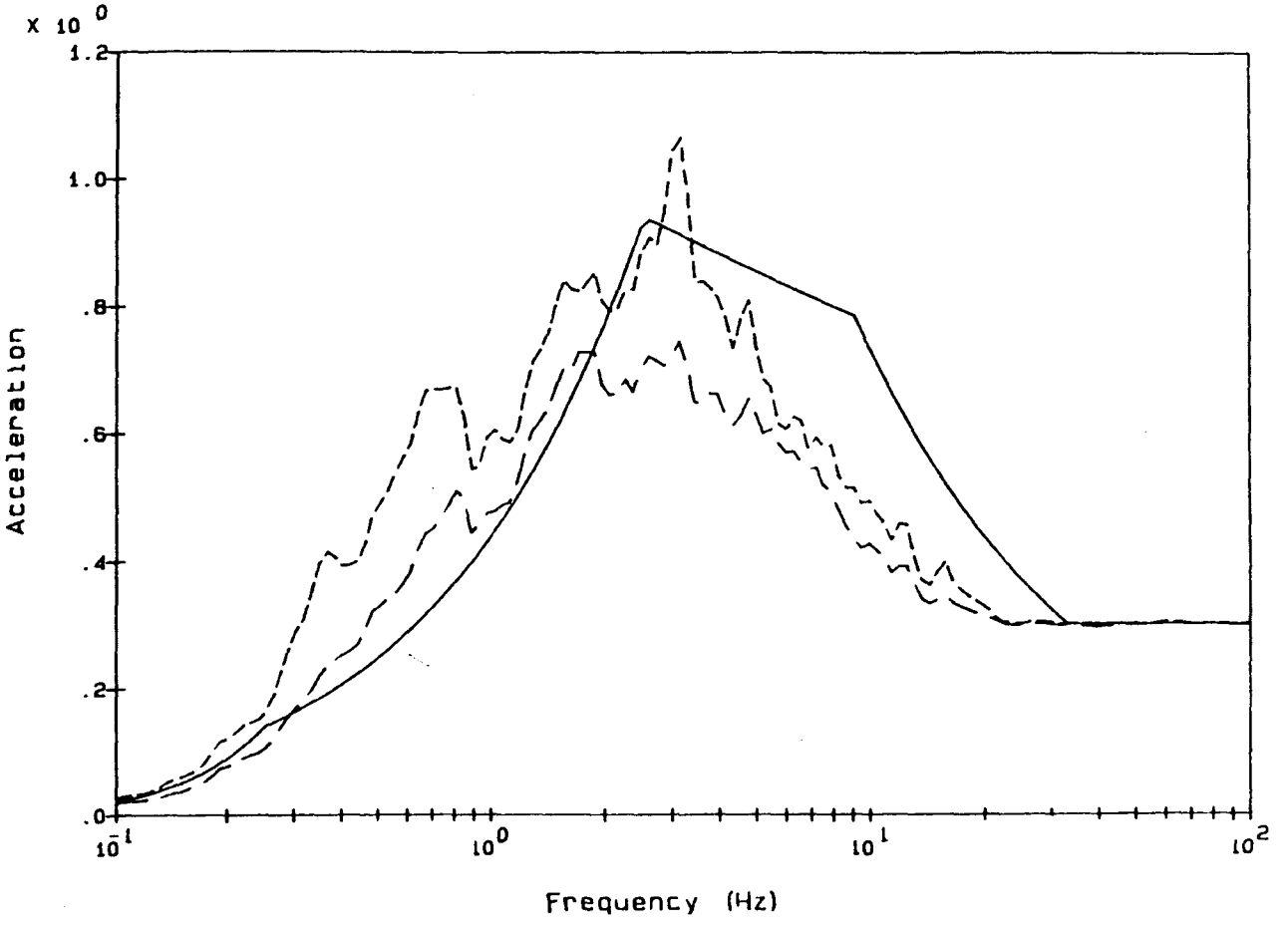

Legend:

A.G.160 horizontal ————————

mean spectrum — — — — .

mean + 1×sigma - - - - - - - - .

Notes:

damping = 5%

accelerations in (g)

scaled to 0.3 g

Fig. 3-3: Mean and Mean-Plus-One-Standard-Deviation Response Spectra at Surface

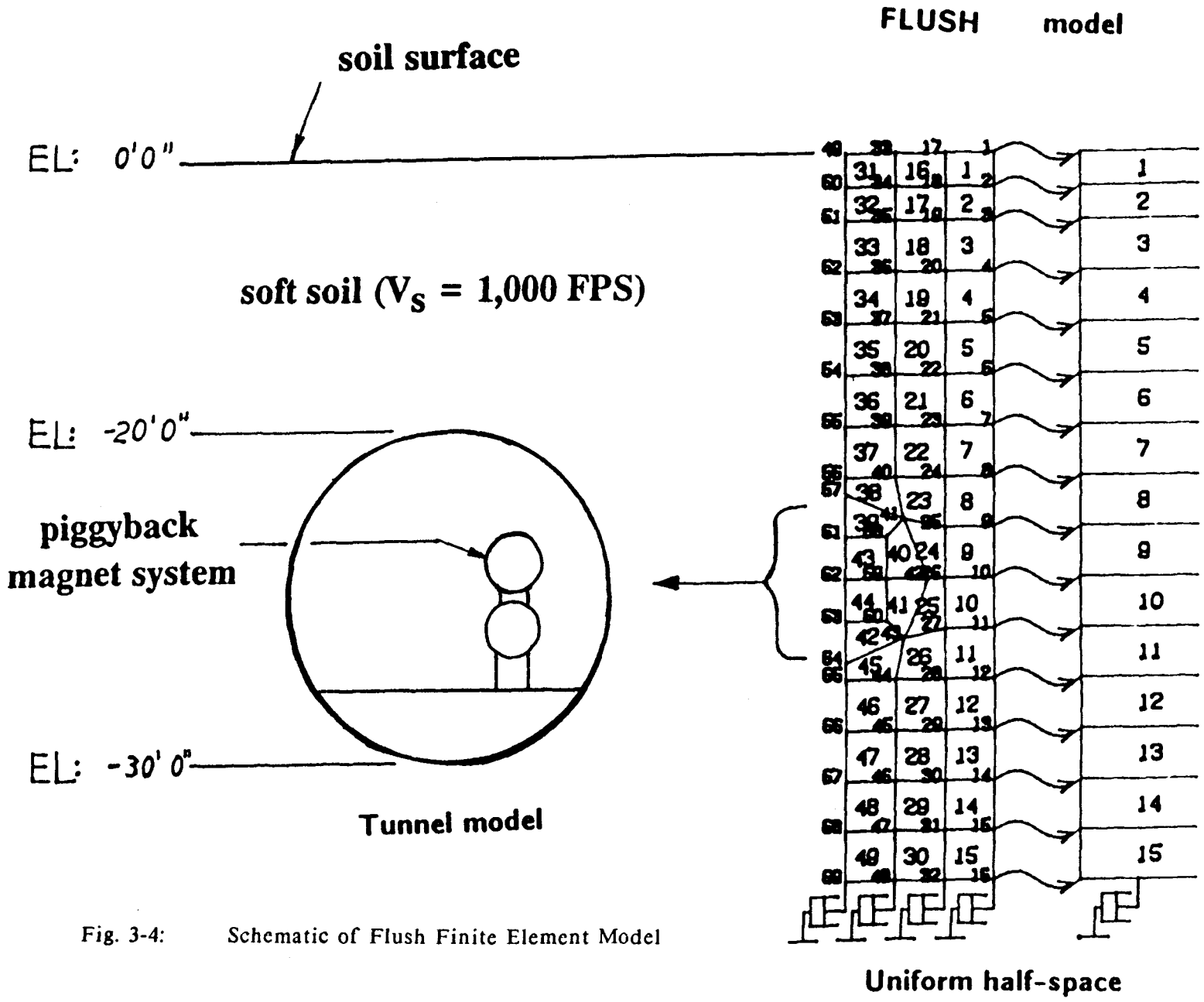

Fig. 3-4: Schematic of Flush Finite Element Model

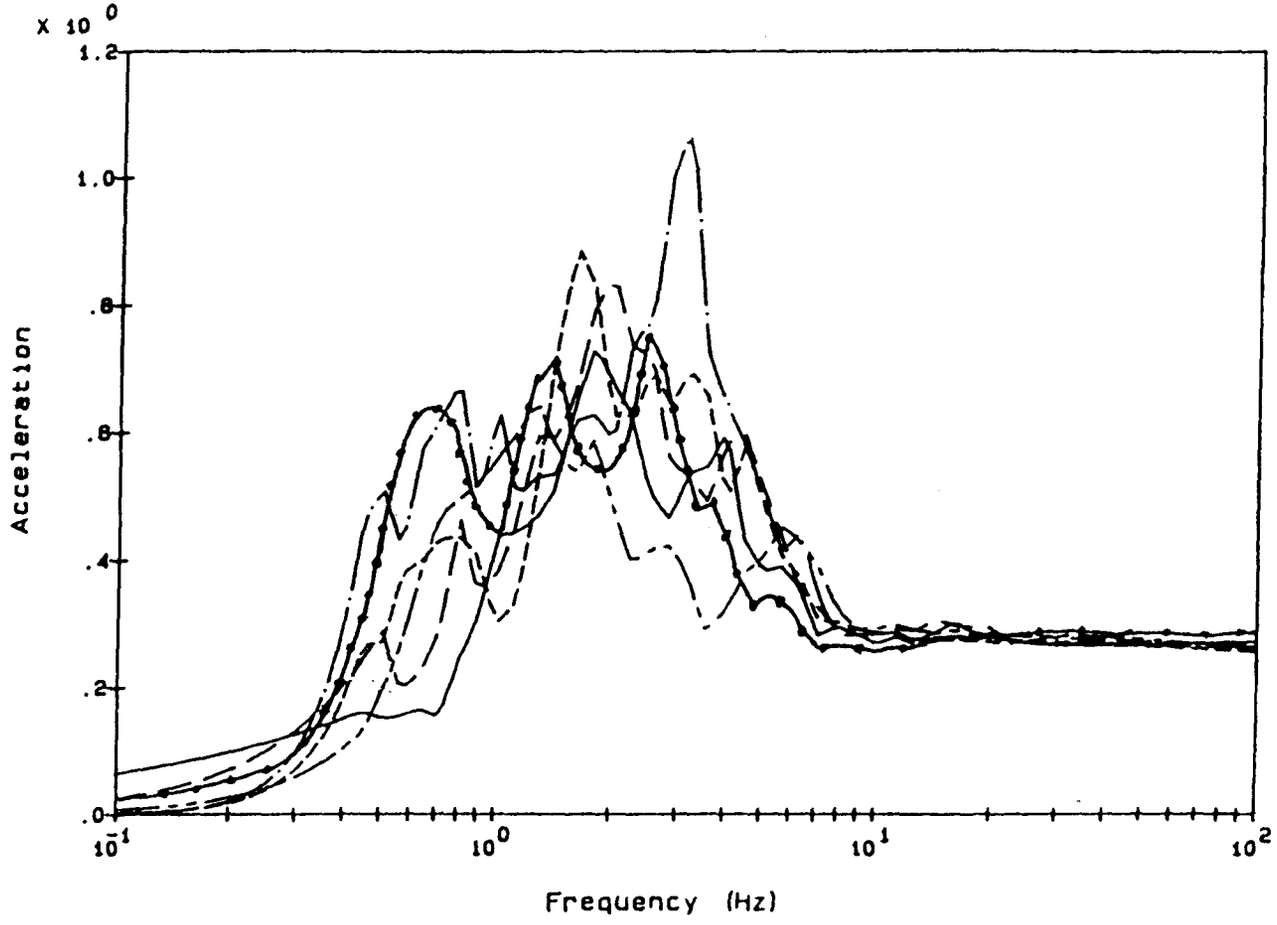

Legend:

El Centro	s00e	————————
El Centro	s90w	— — — — .
San Fernando	n00w	- - - - - - - - - .
San Fernando	s90w	——— . ——— . .
Ferndale	n46w	—— - - —— - - - .
Ferndale	n44e	—•—•—•—•—

Notes:

damping = 5%
accelerations in (g)
scaled to .3g (surf)

Fig. 3-5: Site Specific Response Spectra at -30 ft. (Six Components)

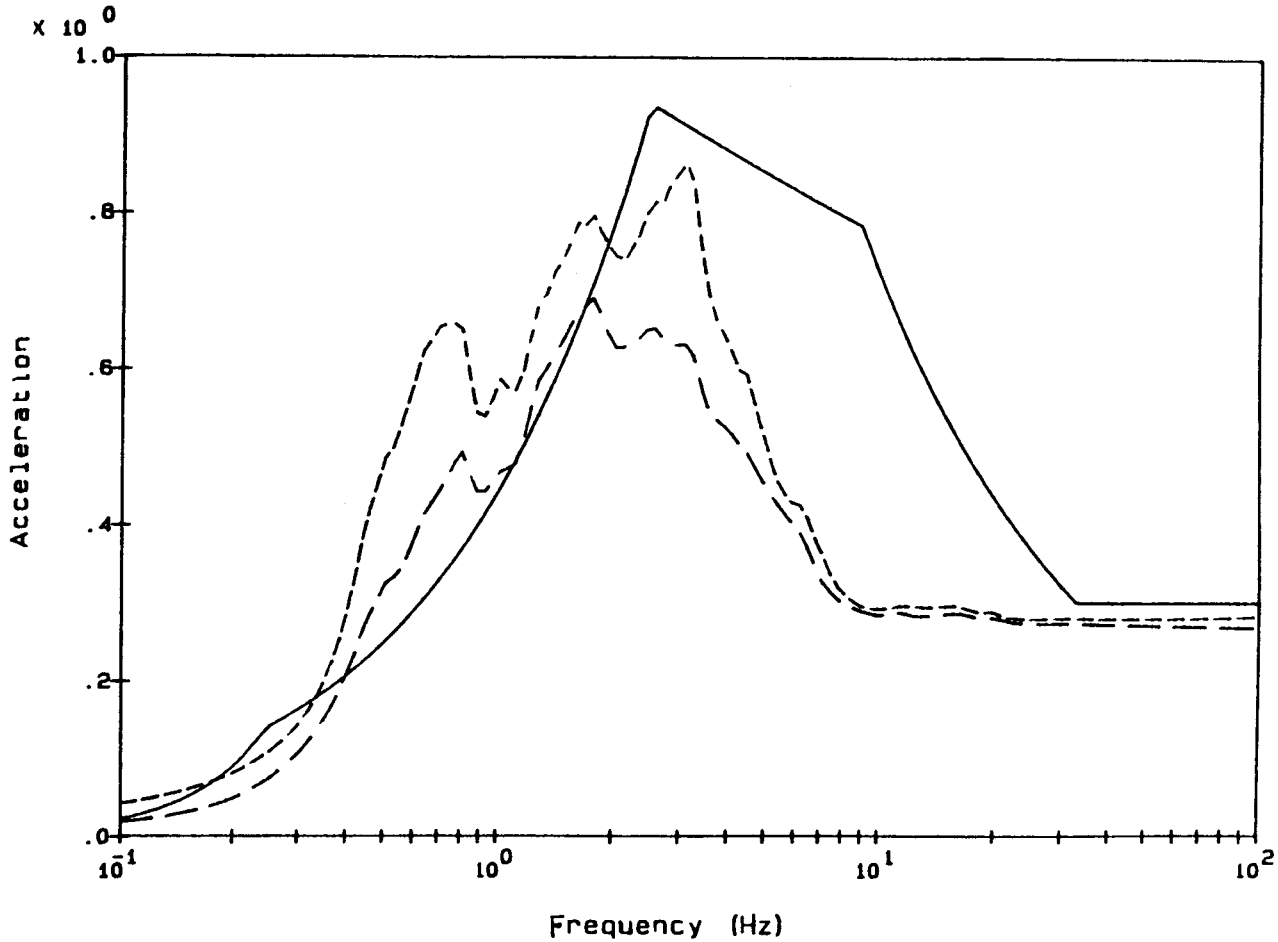

Legend:

R.G.160 horizontal ————————

mean spectrum — — — — .

mean + 1*sigma - - - - - - - - -

Notes:

damping = 5%

accelerations in (g)

scaled to .3g (surf)

Fig. 3-6: Mean and Mean-Plus-One-Standard-Deviation Response Spectra at -30 ft.

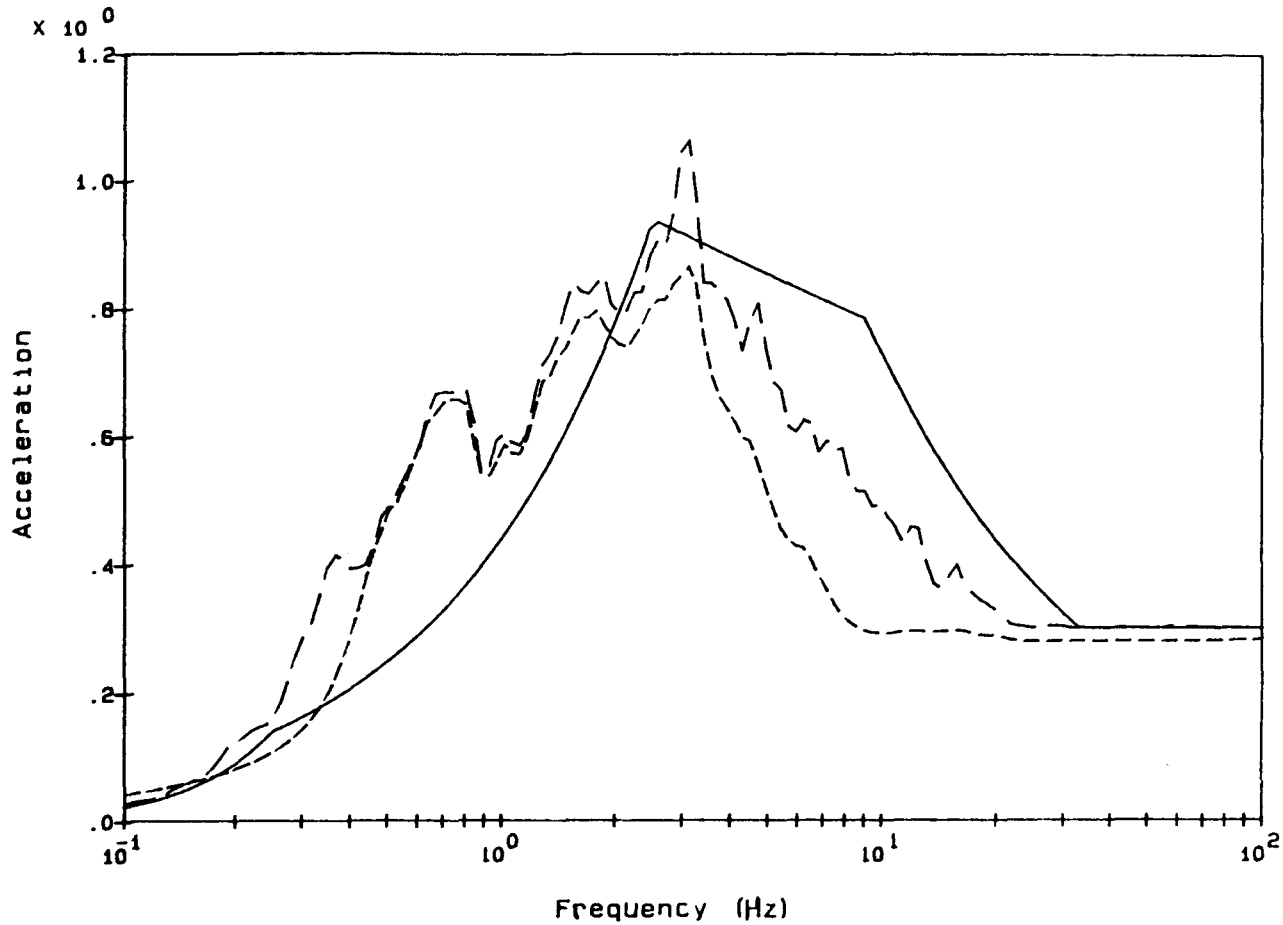

Legend:

R.G.160 horizontal

mean+1*sigma (sur)

mean+1*sigma (-30)

Notes:

damping = 5%

accelerations in (g)

scaled to .3g (surf)

Fig. 3-7: Comparison of Mean Plus-One-Standard-Deviation Spectra with RG 1.60

ENVIRONMENT	AMPLITUDE	DURATION (SEC)	PULSE SHAPE	DIRECTION
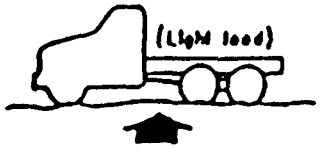	0.6 TO 1.1G	0.0022 TO 0.200	HALF-SINE	VERTICAL
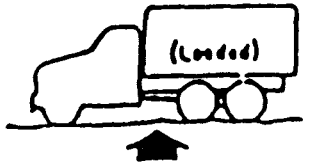	0.3 TO 2.0G	0.0025 TO 0.200	HALF-SINE	VERTICAL
	0.7G	0.084	HALF-SINE	LATERAL
	0.3 TO 0.6G	0.009 TO 0.040	HALF-SINE	LATERAL

Fig. 3-8: Typical Impulse Shock Loads for Various Environments

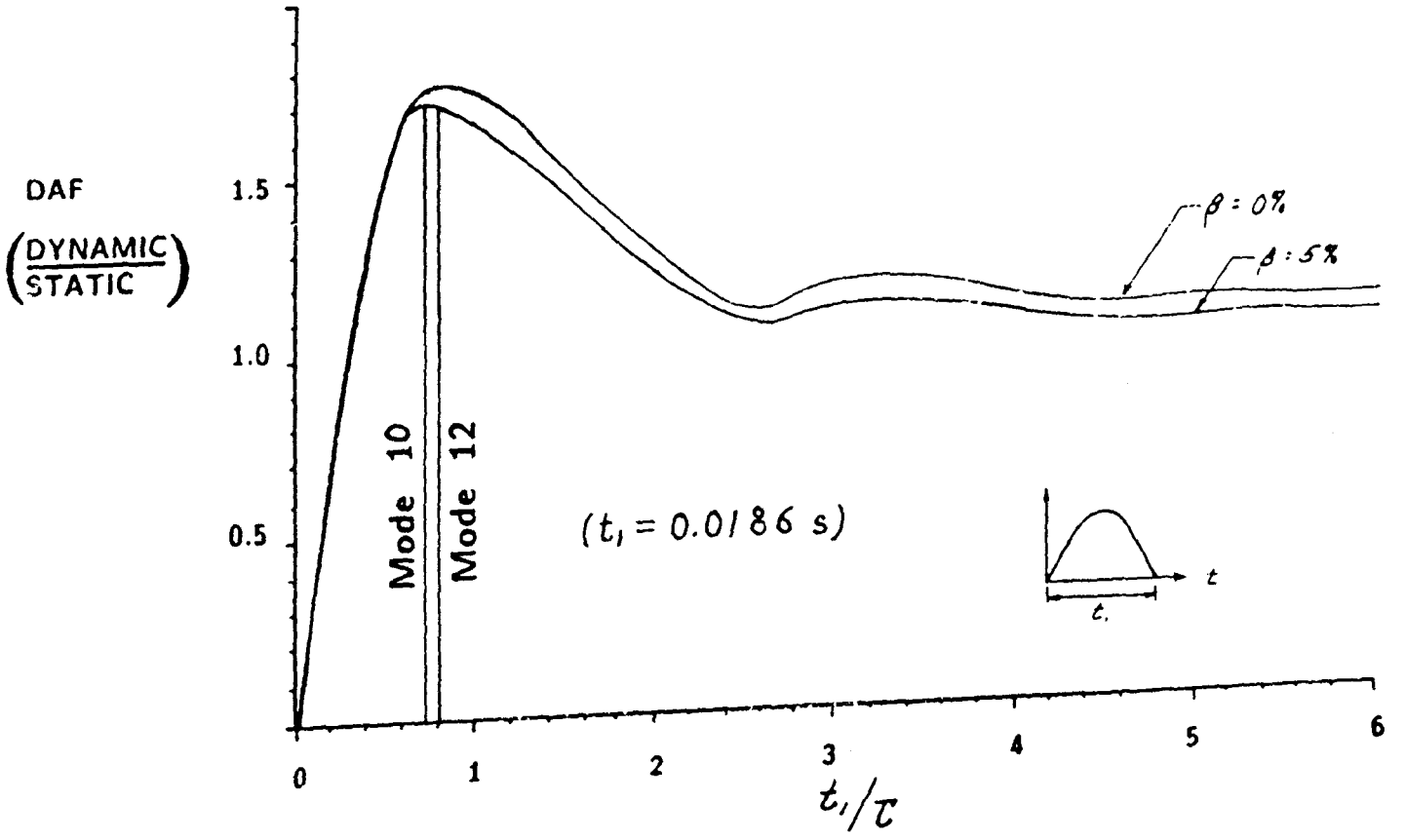

Fig. 3-9: Half-Sine Pulse Reponse Spectrum for Axial Direction

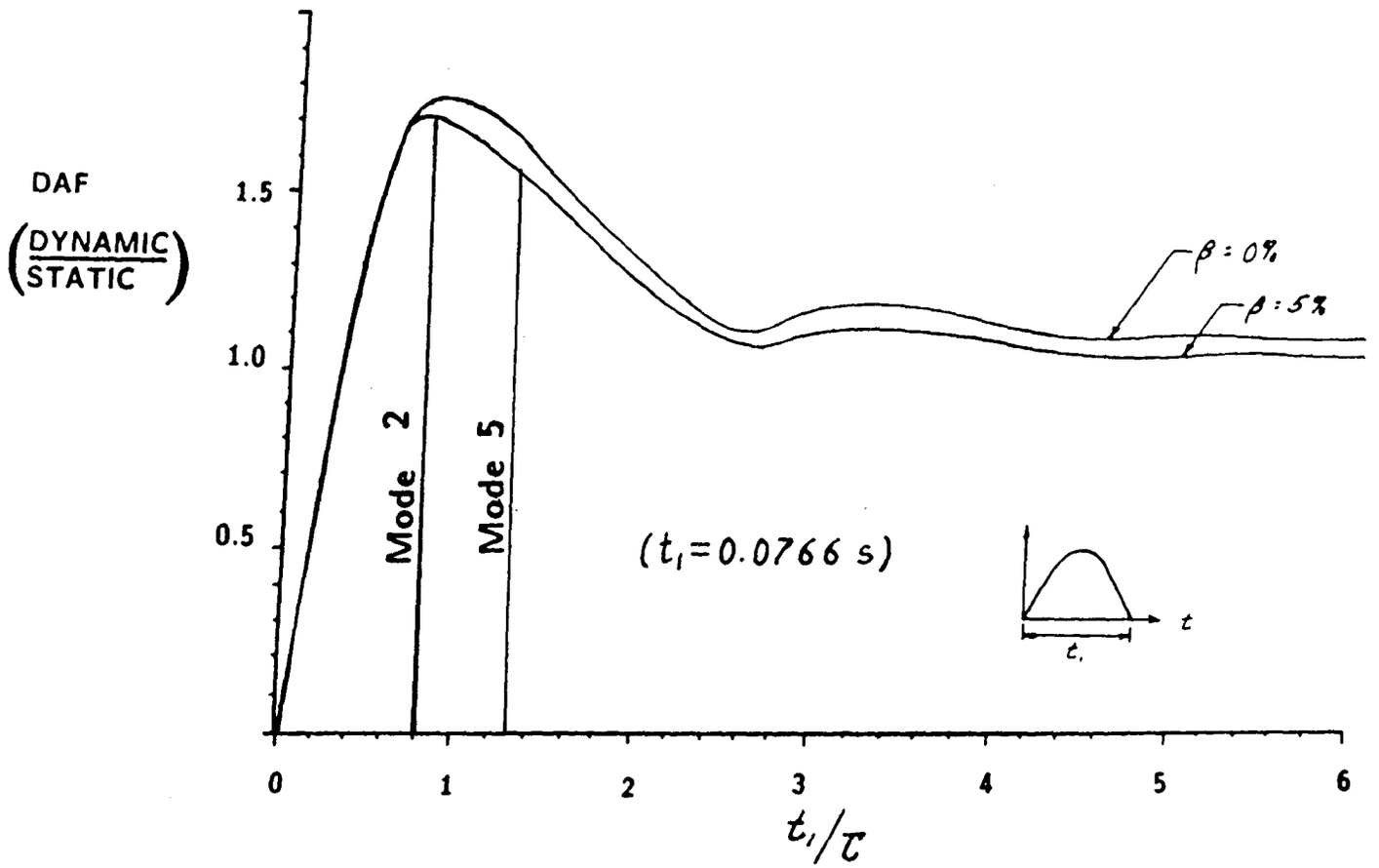

Fig. 3-10: Half-Sine Pulse Response Spectrum for Lateral Direction

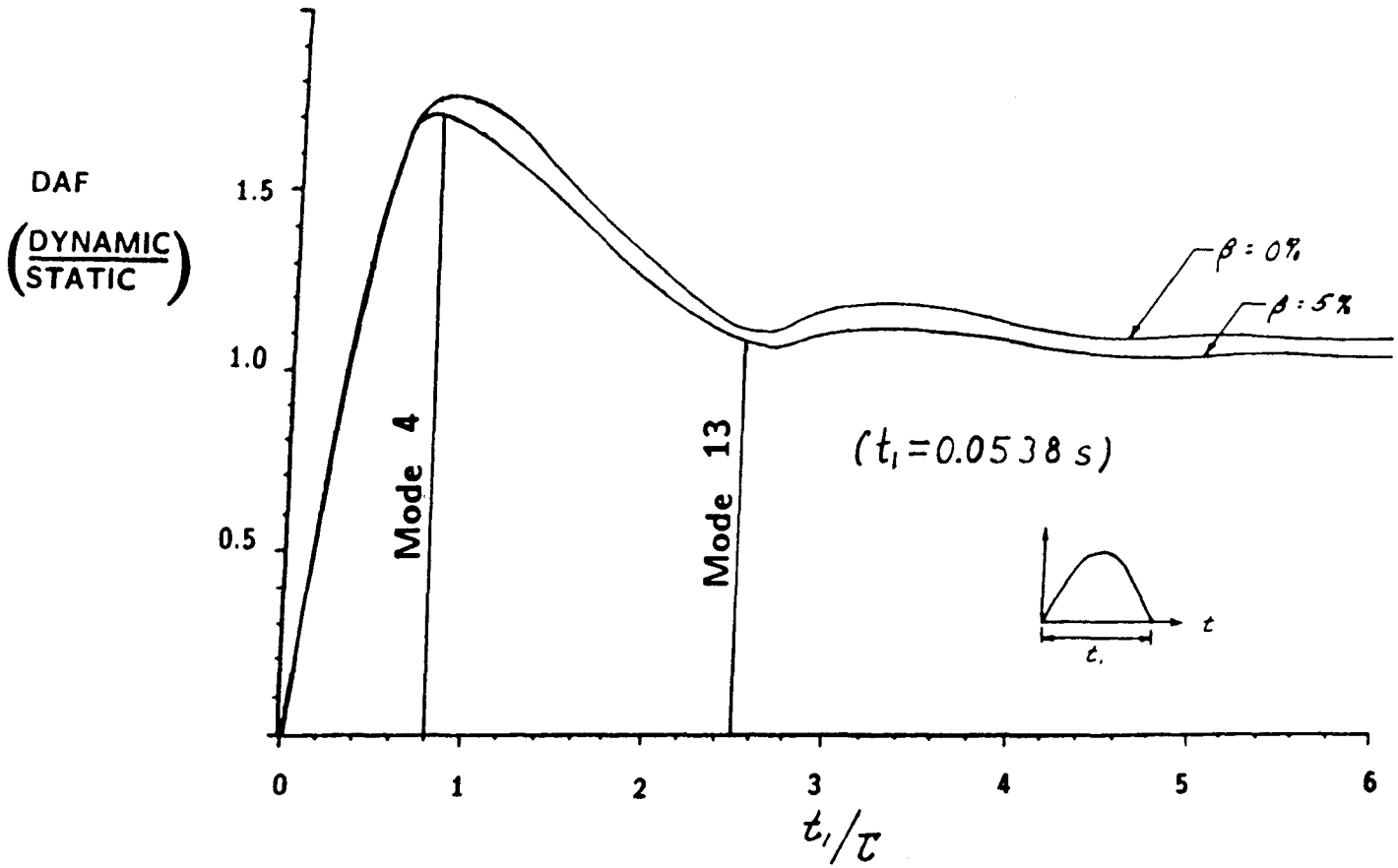

Fig. 3-11: Half-Sine Pulse Response Spectrum for Vertical Direction

4.0 SUMMARY AND RECOMMENDATIONS

4.1 STRESS SUMMARY

Based on the results discussed in Secs. 3.2 and 3.3, the following stress summary is presented.

Cold Mass

For both seismic and transportation loading conditions, very low stresses are induced in the cold mass -- well below allowable values.

Support Posts

For seismic excitations, overstresses in the posts depend on the seismic environment and the configuration of the magnet system. Considering a load combination of seismic and dead load stresses, the following summarizes the maximum ground accelerations that the center post (the most critical) can withstand. Note that these peak values were determined in all cases by the governing lateral excitation. Based on the RG 1.60 design spectra, the single and piggyback configurations can withstand 0.32g and 0.21g PGA respectively. These values increase to 0.44g and 0.25g PGA for the soft soil design spectra and the assembly founded at the ground surface. These values increase further to 0.64g and 0.37g PGA on the soil surface for the configuration founded at a 30 foot depth in the soft soil.

For transportation loading, the center post is overstressed by a factor of two given the listed design allowables and considering once again the pulse load and dead load combination. As was the case for seismic, transportation overstresses are governed by lateral excitations.

Cradles

For both seismic and transportation loading, the outboard and center cradles are stressed below their allowable. The maximum stress in the center cradle is 2.2 ksi and the maximum stress in the outboard cradle is 9 ksi. Therefore no cradle design changes are warranted.

Tie-Bars

Tie bar stresses were very low for both seismic and transportation excitations -- 1 ksi maximum. Therefore, this is not an area of concern.

4.2 RECOMMENDATIONS

Allowable Stresses and Load Combinations

A review of the allowable stresses and load combinations specified in Ref. 1 is essential before one can draw firm conclusions on the capacity of the system to withstand seismic and transportation loading conditions. This review of allowable stresses is necessary to remove excess conservatism if it exists. A review of load combinations is essential for two purposes. First, to verify that the loading combinations specified are not overly conservative, i.e., if relatively low probability events of substantial consequences are specified for load combination, the appropriateness of their combination should be verified. Second, to establish the seismic capacity of the vacuum vessel and magnet system, stresses induced by all specified loading conditions need to be combined.

Piggyback Configuration

As discussed in Sec. 4.3, a design modification to stiffen the vacuum vessel connecting ring for the upper magnet system will increase the seismic capacity of the upper magnet system approaching that of the lower magnet system. This stiffened connecting ring should be designed, its stiffness calculated, and the piggyback configuration re-analyzed.

Site Conditions

The present evaluation was performed for a generic site-independent response spectra (RG 1.60) assuming the system to be surface-founded and for a generic soft soil site assuming the system to be surface founded and at a 30 foot depth in the soil. Both cases are extremely informative in establishing the seismic capacity of the system. However, when actual potential sites are identified, their seismicity and site specific characteristics need to be evaluated.

Connection Bolts

A critical assumption made at the onset of these analyses involves the boundary condition at the base of the lower vacuum vessel support rings. We assumed the support connection fixed at the base in all directions. In order to ensure this to be

valid, we recommend that preloaded bolts be used at these locations such that a sufficiently large torque may be applied to keep the base plate flush with the concrete support pad. Also, the connection between lower and upper support rings was assumed to behave similarly for the piggyback configuration. Therefore, all bolts used in restraining the support rings should be preloaded.

4.3 POTENTIAL DESIGN MODIFICATIONS

Stiffen Connecting Ring for Seismic Excitation

During seismic excitation, posts in the upper magnet of the piggyback configuration experience critical overstresses which could easily be avoided by stiffening the two vacuum vessel support rings laterally. This would involve extending the existing stiffeners out to the diameter of the ring at the waist and thickening them. The welding process is already required for these stiffeners and this modification would simply be an extension of that task. This modification would also preserve the maximum width of the support as designed.

Lateral Transportation Restraints

The results for the transportation model in the lateral direction indicate that at least a temporary restraint be inserted into the vacuum vessel to transfer lateral stresses through the connecting rings to the base support instead of transferring it all through the posts. Indeed this would create fabrication and handling difficulties depending on where inside the vessel these restraints are placed. Restraints would not necessarily need to be placed at all post locations, but probably at least the two intermediate outer posts (second and fourth). Further investigation would be necessary to assess the feasibility and effectiveness of this modification.

5.0 REFERENCES

1. "SSC Collider Magnet System Requirements-II." General Requirements: Issue No.2, July 21, 1987.

2. Craddock, W., "Measurement of the Flexural Rigidity of the SSC Heat Leak Model #2," Informal Memo, Fermi National Accelerator Laboratory, February 3, 1986.

3. Johnson, J. J., "MODSAP -- A Modified Version of the Structural Analysis Program SAP IV for the Static and Dynamic Response of Linear and Localized Nonlinear Structures," General Atomic Company, GA - A 14006, June 1978.

4. Algor Interactive Systems, Inc., "SUPERSAP - Finite Element Stress and Dynamic Analysis Software," 1986.

5. Murray, R., "GEMINI - A Computer Program for Two and Three Dimensional Linear Static and Seismic Structural Analysis," UCID - 203398, October, 1984.

6. Bernreuter, D. L., Personal Communication with Johnson, J. J., July, 1987.

7. Udaka, T., "SUPERFLUSH -- Strain Dependent, Equivalent Linear Finite Element Program for Efficient Seismic Soil Structure Interaction Analysis," 1986.